Physiologic and Genomic Analyses of Nutrition-Ethanol Interactions During Gestation: Implications for Fetal Ethanol Toxicity

KARTIK SHANKAR,*,‡ MATS HIDESTRAND,*,‡ XIAOLI LIU,*,‡ RIJIN XIAO,†,‡ CHARLES M. SKINNER,‡ FRANK A. SIMMEN,†,‡ THOMAS M. BADGER,*,†,‡ AND MARTIN J. J. RONIS*,‡,[1]

*Departments of *Pharmacology and Toxicology and †Physiology and Biophysics, University of Arkansas for Medical Sciences, Little Rock, Arkansas 72205; and ‡Arkansas Children's Nutrition Center, Little Rock, AR, 72202*

Nutrition-ethanol (EtOH) interactions during gestation remain unclear primarily due to the lack of appropriate rodent models. In the present report we utilize total enteral nutrition (TEN) to specifically understand the roles of nutrition and caloric intake in EtOH-induced fetal toxicity. Time-impregnated rats were intragastrically fed either control or diets containing EtOH (8–14 g/kg/day) at a recommended caloric intake for pregnant rats or rats 30% undernourished, from gestation day (GD) 6–20. Decreased fetal weight and litter size ($P < 0.05$) and increased full litter resorptions (33% vs. 0%), were observed in undernourished dams compared to adequately fed rats given the same dose of EtOH, while undernutrition alone did not produce any fetal toxicity. Undernutrition led to impairment of EtOH metabolism, increased blood EtOH concentrations (160%), and decreased maternal hepatic ADH1 mRNA, protein, and activity. Microarray analyses of maternal hepatic gene expression on GD15 revealed that 369 genes were altered by EtOH in the presence of undernutrition, as compared to only 37 genes by EtOH *per se* (±2-fold, $P < 0.05$). Hierarchical clustering and gene ontology analysis revealed that stress and external stimulus responses, transcriptional regulation, cellular homeostasis, and protein metabolism were affected uniquely in the EtOH-undernutrition group, but not by EtOH alone. Microarray data were confirmed using real-time RT-PCR. Undernourished EtOH-fed animals had 2-fold lower IGF-1 mRNA and 10-fold lower serum IGF-1 protein levels compared to undernourished controls ($P < 0.0005$). Examination of maternal GH signaling *via* STAT5a and -5b revealed significant reduction in both gene and protein expression produced by both EtOH and undernutrition. However, despite significantly elevated fetal BECs, fetal IGF-1 mRNA and protein were not affected by EtOH or EtOH-undernutrition combinations. Our data suggest that undernutrition potentiates the fetal toxicity of EtOH in part by disrupting maternal GH-IGF-1, signaling thereby decreasing maternal uterine capacity and placental growth. Exp Biol Med 231:1379–1397, 2006

Key words: ethanol; pregnancy; fetal alcohol syndrome; microarray; undernutrition

Introduction

The fetotoxic potential of ethanol (EtOH) has been recognized for nearly three decades, but EtOH continues to be the most common teratogen ingested during pregnancy (1). One of every 29 women who know they are pregnant report EtOH consumption (2). The toxic effects of EtOH are manifested by a constellation of physical, behavioral, and cognitive abnormalities commonly referred to as Fetal Alcohol Spectrum Disorder (FASD). In addition to mental retardation, *in utero* EtOH exposure results in increased rates of miscarriage, reduced birth weight, growth retardation, and teratogenic effects (3). The incidence of FASD in the general U.S. population ranges from 0.7 to 10 cases per 1000 live births annually (2), which is still a surprisingly small proportion of all children exposed to EtOH during fetal development. The reasons for the low penetrance of FASD and precise mechanisms causing FASD remain elusive. However, it is established that EtOH interferes with nutritional supply to the fetal-placental unit (4). Inadequate maternal diets have been demonstrated to exacerbate the effects of ethanol, and women who consume EtOH during pregnancy are often also malnourished (5). Moreover, chronic EtOH consumption can directly or indirectly

These studies were supported in part by R01AA012819 to M.J.J.R.

[1] To whom correspondence should be addressed at Arkansas Children's Nutrition Center, Slot 512–20B, 1120 Marshall Street, Little Rock, AR 72202. E-mail: RonisMartinJ@uams.edu

Received January 9, 2006.
Accepted March 24, 2006.

1535-3702/06/2318-1379$15.00

compromise nutritional status. Undernutrition resulting in low prepregnancy weight and low gestational weight gain is reported to be a significant independent risk factor for adverse pregnancy outcomes. Hence it is clear from the literature in this area that nutritional aspects of prenatal EtOH exposure are of fundamental importance in determining the toxic effects of EtOH.

Rats administered EtOH *via* liquid diets (Lieber-Decarli) are often undernourished, consuming as much as 25%–40% less calories than controls fed *ad libitum* (6, 7). Inadequate nutrition is a particular problem in studies of EtOH consumption during pregnancy due to the increased nutritional requirements imposed by the growing fetal-placental unit. Feeding early formulations of the Lieber-DeCarli diets to pregnant rodents resulted in a 30%–50% reduction in gestational weight gain in pair-fed compared to *ad libitum*–fed dams (6, 8). While newer formulations of the Lieber-DiCarli diet result in improved body weight gains during gestation, significant deficits persist (8, 9). Lower weight gains during pregnancy are in good part related to decreased dietary intake and independent of EtOH consumption (6). In order to dissect the effects of EtOH and undernutrition in pregnancy on adverse outcomes, we have utilized intragastric infusion models in which isocaloric EtOH-containing liquid diets are administered directly into the stomach *via* an enteral cannula (10–12).

Previous studies have demonstrated that pregnant rats fed nutritionally adequate diets (220 kcal/day/kg$^{3/4}$) containing the same dose of EtOH as nonpregnant rats, have significantly greater EtOH metabolism and consequently lower blood ethanol concentrations (BEC) (13). Hence pregnancy tends to provide a degree of protection against EtOH fetal toxicity by enhancing its metabolism and reducing the dose of EtOH reaching target tissues. The present study had three objectives. The first objective was to examine the role of caloric intake on EtOH metabolism in pregnancy. We hypothesized that adequate nutrition is essential for pregnancy-induced enhancement of EtOH metabolism. The second objective was to determine the effect of increasing doses of EtOH on fetal toxicity while maintaining adequate nutrition during pregnancy. Thirdly, these studies aimed to ascertain if undernutrition synergizes with the toxic effects of EtOH. To examine the mechanistic basis of how nutrition and EtOH produce interactive toxicity, we examined the status of ethanol-metabolizing enzymes, alcohol dehydrogenase (ADH), aldehyde dehydrogenase (ALDH), and microsomal CYP2E1. Furthermore, microarray-based gene expression analyses of maternal liver were carried out to identify unique changes and novel mechanisms. Modulation of insulin-like growth factor 1 (IGF-1) and insulin-like growth factor binding protein 1 and 2 (IGFBP-1 and -2) were studied. Our data strongly suggest that inadequate nutrition significantly increases fetal EtOH toxicity by impairing maternal EtOH metabolism and may also disrupt GH-IGF-1 signaling in the maternal axis.

Materials and Methods

Animals and Experimental Protocol. Unless otherwise specified, all chemicals were obtained from Sigma-Aldrich Chemical Co. (St. Louis, MO). Time impregnated female Sprague-Dawley rats (250–300 g) and weight-matched nonpregnant cohorts were obtained from Charles River Laboratories (Wilmington, MA). Animals were housed in an AAALAC-approved animal facility, and animal maintenance and experimental treatments were conducted in accordance with the ethical guidelines for animal research established and approved by the Institutional Animal Care and Use Committee (IACUC). Rats were surgically cannulated with intragastric cannulae and infused either control or EtOH-containing diets, as described previously (10, 11). Rats were briefly anesthetized with Nembutal (50 mg/kg, ip) and reflexes, breathing, and skin color were monitored. The stomach was exposed and a cannula (0.025 in. i.d. × 0.45 in. o.d.) was inserted and secured with a suture at the interface between the cardiac and pyloric regions. The free end of the cannula was threaded subcutaneously to a headpiece that was anchored on the skull with acrylic dental cement. A swiveled spring acted as a tethering device and was attached to the dental cement. This allowed complete, unrestrained 360° movement for the rats. All animals were infused diets at a constant rate between 1800 and 0800 hrs (during the dark cycle). Animals had access to unlimited water throughout the experiment.

Experimental Treatments: Study 1. To examine if pregnancy-induced changes in EtOH metabolism are dependent on the level of nutritional intake, nonpregnant and pregnant rats were divided into two groups. Time-impregnated female Sprague-Dawley rats (300 g) were obtained on Day 4 of gestation (GD4) and allowed to acclimatize in our facility for 1 day. On GD5, an intragastric cannula was surgically inserted into pregnant and nonpregnant rats ($n = 4$–5) and infused with EtOH-containing diets (EtOH, 13 g/kg/day, carbohydrate isocalorically replaced by ethanol) as described previously (10, 11). Two levels of caloric intake were administered to nonpregnant and pregnant rats, 220 kcal/day/kg$^{3/4}$ (the caloric intake recommended for pregnant rats by the National Research Council, NRC) and 160 kcal/day/kg$^{3/4}$ (undernourished), keeping minerals and vitamins at NRC-recommended levels while reducing all macronutrient components equally. Since urine ethanol concentrations (UECs) have been observed to be excellent predictors of blood ethanol concentrations in both cycling and pregnant rats (10, 11), 24-hr UECs were measured daily for 15 days using the Analox Instruments GL5 Analyzer fitted with an amperometric oxygen electrode sensor (Analox Instruments Ltd., London, UK).

Study 2. To examine if ethanol-induced fetal toxicity increases with dose, groups of time-impregnated female Sprague-Dawley rats (300 g) were delivered to our animal

facility on GD4 and cannulated and fed as described above. The EtOH dose was 0, 8, 9, 10, 10.75, 11.8, 13, or 14 g/kg/day for groups of animals fed 220 kcal/kg$^{3/4}$/day, achieved by isocalorically substituting EtOH for carbohydrate calories. Twenty-four hour UECs were measured daily (as described above) from GD6–7 to GD20. At GD20, dams (n = 3–15) were euthanized with 100 mg/kg Nembutol and the fetuses were counted, dissected, and weighed. Uteri were stained with 10% ammonium sulfide to verify embryonic implantation.

Study 3. To determine if maternal undernutrition potentiates EtOH toxicity, one group of time-impregnated rats was fed 220 kcal/ kg$^{3/4}$/day and the other group was calorically restricted at 160 kcal/ kg$^{3/4}$/day (n = 7–8). Both groups received 13 g/kg/day of EtOH, and 24 hour UECs were analyzed. At the end of this experiment on GD20, dams were sacrificed and fetal effects and litter numbers were evaluated as described in Study 2. In addition, activities of the major alcohol metabolizing enzymes, ADH, ALDH, and CYP2E1, were measured in maternal liver.

Study 4. Finally, to assess the relative contributions of adequate maternal nutrition and *in utero* ethanol exposure on fetal toxicity parameters and to examine the role of maternal IGF-1 in fetal growth retardation, time-impregnated rats were infused control or EtOH-containing TEN diets at 220 kcal/kg$^{3/4}$/day or 160 kcal/kg$^{3/4}$/day from GD6–GD15. The EtOH dose was 12 g/kg/day and was substituted for isocaloric amount of carbohydrate in control diets. UECs were measured daily as described above. On GD15, all dams were sacrificed under anesthesia and serum, livers (maternal), and fetuses were collected. Litter size, weight, and the number of total litter resorptions were recorded. Livers were flash-frozen in liquid nitrogen and stored at −70 °C.

In a separate experiment, dams were fed throughout gestation using the same paradigm as described in Study 4, but continued until GD20. On GD20, all dams were sacrificed under anesthesia and maternal and fetal serum and livers were collected. Serum from all fetuses belonging to one dam were pooled and frozen. Livers were flash-frozen in liquid nitrogen and stored at −70 °C. Amniotic fluid was also pooled from several placental sacs per dam and frozen for EtOH concentration analysis.

Hepatic Alcohol Dehydrogenase and Aldehyde Dehydrogenase Activities. Liver homogenates from flash frozen livers were prepared in phosphate-sucrose buffer containing 1% Triton X-100 and 1 mM mercaptoethanol and centrifuged at 10,000 g for 30 mins. Supernatants were assayed for ADH and ALDH activities by measuring the formation of NADH at 340 nm (14). ADH (EC 1.1.1.1) activity was assayed at pH 8.5 in pyrophosphate-glycine buffer with 50 mM ethanol and 1 mM 4-methylpyrazole in the reference cuvette. ALDH (EC 1.2.1.3) was measured at pH 8.8 in the presence of 0.5 mM 4-methylpyrazole and 1 mM mercaptoethanol using 0.5 mM acetaldehyde as substrate (14).

Hepatic Microsomal CYP2E1 Activity. Liver microsomes were prepared from livers of EtOH-fed dams by differential ultracentrifugation. Protein concentration of the microsomes was determined by the Bradford method using the Bio-Rad Protein Assay (Bio-Rad, Hercules, CA). Microsomes were stored at −70° C. Microsomal CYP2E1 activity was assayed by measuring carbon tetrachloride–dependent lipid peroxidation (15).

Quantitation of Hepatic ADH-1, STAT5a, and STAT5b Proteins by Western Blotting. Hepatic cytosolic fractions were resolved on polyacrylamide gels and transferred to PVDF membranes (Bio-Rad). Immunoblotting was carried out using standard procedures, as previously described (16). Membranes were incubated with primary antibodies for ADH-1, STAT5a, and STAT5b (rabbit anti-rat ADH-1 [16], STAT5a, and STAT5b [1:1000; Upstate Biotechnology, Chicago, IL]) in TBST containing 5% milk powder for 1 hr at room temperature. Following incubation with HRP-conjugated secondary IgG (1:10,000), membranes were washed with TBST and proteins visualized using West Pico ECL chemiluminescence kit (Pierce, Rockford, IL) and detected by autoradiography. Immunoquantitation was performed by densitometric scanning of the resulting autoradiograms using a Bio-Rad GS700 molecular imager.

Hepatic Gene Expression Analysis. *Microarray-Based Analyses.* Hepatic gene expression profiles were assessed using Affymetrix RGU34A GeneChip microarrays (Affymetrix, Santa Clara, CA) containing 8800 genes, with approximately 7000 full-length transcripts and 1800 EST sequences. Livers were excised from dams fed control or EtOH diets (n = 3–4) from GD6 through GD15 containing 220 kcal/kg$^{3/4}$/day or 160 kcal/kg$^{3/4}$/day. Total RNA was extracted from livers using TRI reagent and cleaned using RNeasy mini columns (Qiagen, Valencia, CA). RNA quality was ascertained spectrophotometrically (ratio of A_260/A_280) and also by checking ratio of 18S to 28S ribosomal RNA using the RNA Nano Chip on a 2100 Bioanalyzer (Agilent Technologies, Palo Alto, CA). Sample preparation and hybridizations (from individual animals, n = 3–4 per group) were carried out using manufacturer's instructions. Microarrays were scanned using an Agilent microarray scanner. Raw data intensities acquired from the .cel files using Microarray Suite 5.0 software (Affymetrix) were globally normalized using scaling factor normalization. Genes were filtered based on presence/absence call (either 2 out of 3 or 3 out of 4), and average ± SEM gene expression for each treatment group was computed for present genes. For comparison analysis, genes were filtered based on minimum 2-fold ratio change and P value (<0.05) using Student's t test. Data analyses were performed using Microsoft Excel and SpotFire DecisionSite for Functional Genomics. Correlation based hierarchical clustering between treatment groups was done using Cluster software

Table 1. Primers sequences for real-time RT-PCR analyses[a]

Gene Name	Forward primer (5′–3′)	Reverse primer (5′–3′)
IGF-1	ACTTTCTTTCCGTGCTGGGTC	GAGTACAAAGCCAGCCTGTGC
IGF-2	GTCGATGTTGGTGCTTCTCATCT	CGGTCCGAACAGACAAACTGAA
IGFBP-1	AGATTAGCTGCCGCTCAACAGA	GTCTCGCACTGTTTGCTGTGAT
IGFBP-2	CCTGCATATCCCCAACTGTGA	CTGGATTGGCTTCCCAGTATTG
IGFBP-4	ATTGATGCACGGGCAAGGT	AGCTGTTGTTGGGATGCTCACT
Stat 5a	ATTCAGCGACTCGGAAATCG	GAGAAATCCCGAGTGGTGAATG
Stat 5b	CAGTTCAGTGTTGGTGGAAATGAG	GGTAGCCGTCGCATTGTTGT
ADH-1	CACCAAACCCATCCAGGAAGT	GCATGCTGAATGGCAGCTTAA
Glucokinase	CTGACTTCCTTGACAAGCATCAGA	GAGGATGCCCTTGTCTAGGTCTTC
Phosphoenolpyruvate carboxykinase	AACCCCGAAGGCAAGAAGAA	CACCCACACATTCAACTTTCCA
Fas ligand	AAAGTCGAAGCCGCACTGAA	TGGTTGGGAACCACAAAACTG
Cyclooxygenase 1	AGCAGGGATACCTCGTCGTTACT	GCGAAGGCTTCTCAAATCATGA
Mitochondrial cytochrome B	CCACATCTGCCGAGACGTAAAC	CTCGTCCCACATGGAGGAATAG
Prolactin receptor	GTGTGGATCATTGTGGCCATTC	GGTGGAAAGATGCAGGTCATCA
CD36 antigen	GGCTGTGTTTGGAGGCATTCT	CCCGTTTTCACCCAGTTTTTG
Metallothionein 1	AGCTCCTGCGGCTGCAA	CTTGTCCGAGGCACCTTTG
Metallothionein 2	GCAAGAAAAGCTGCTGTTCCT	GTCCGAAGCCTCTTTGCAGAT
Rev-erbA alpha	CCCCCGGAAGTCTACAAGTG	ACACAGTAGCACCATGCCGTTA
Rev-erbA beta	ACCCCATAGAGGAGAACGGATT	GATGCTGCTGGCTCTCACTACA
Period	GGGCATTACCTCCGAGTATATTGTG	AAGGCGTCCTTCTTACAGTGAAAG
18S rRNA	CCTGTAATTGGAATGAGTCCACTTT	ATACGCTATTGGAGCTGGAATTACC

[a] Gene specific primers were designed using Primer Express Software (Applied Biosystems, Foster City, CA). Real-time PCR reactions were carried out according to manufacturer's instructions for 2X SYBR Green master mix and monitored on an ABI Prism 7000 sequence detection system (Applied Biosystems, Foster City, CA) as described in Materials and Methods.

(17). A companion software, TreeView, was used for the presentation of data (http://rana.lbl.gov/EisenSoftware.htm). Known biological functions of genes were queried and acquired from Affymetrix online data analysis resource NetAffx (http://www.affymetrix.com/analysis/index.affx) and gene ontology analyses performed using GO Browser (Affymetrix). To analyze and identify relationship of genes and known signaling pathways, commercially available PathwayAssist software (Ariadne Genomics, Rockville, MD) was used. Confirmation of microarray gene expression data was done by real-time RT-PCR.

Real-Time RT-PCR. Livers were excised from dams (or fetuses) fed control or EtOH diets ($n = 4$–10) from GD6 through GD15 (or GD20 for fetal livers) containing 220 kcal/kg$^{3/4}$/day or 160 kcal/kg$^{3/4}$/day. Total RNA was extracted from livers as previously described. One μg of total RNA was reverse-transcribed using the IScript Reverse Transcription kit (Bio-Rad) according to manufacturer's instructions. Twenty ng of the reverse transcribed cDNA was utilized for *real-time* PCR using the 2X SYBR Green master mix and monitored on an ABI Prism 7000 sequence detection system (Applied Biosystems, Foster City, CA). Gene-specific probes were designed using Primer Express Software (Table 1; Applied Biosystems). The relative amounts of gene expression were quantitated using a standard curve according to manufacturer's instructions.

Free IGF-1 Radioimmunoassay. Serum from dams (or fetuses) on control or EtOH diets from GD6 through GD15 (or GD20) were analyzed for free IGF-1 using radioimmunoassay (Diagnostic Systems Laboratories, Webster, TX). Prior to immunoradiometric assessment, free IGF-1 was separated from serum samples as described by Lang *et al.* (18). Briefly, serum samples were diluted 1:5 with Krebs-Ringer bicarbonate buffer (pH 7.4) containing 5% bovine serum albumin. The samples were then centrifuged at 300 *g* at 37°C using Amicon Centrifree YM-30 tubes (Millipore Corporation, Bedford, MA) for 100 mins. The ultrafiltrate from 40 to 100 mins of centrifugation was used for free IGF-1 analyses. The radioimmunoassay for free IGF-1 was carried out according to manufacturer's instructions.

Data and Statistical Analysis. Data are expressed as means ± SEM. Quantitation of Western blot autoradiograms was performed using Quantity One software (Bio-Rad). SigmaStat software package version 3.0 (SPSS Inc., Chicago, IL) was used to perform all statistical tests. The data were tested using Levene's test for equality of variance. Pearson product moment correlation was performed using SigmaStat software. Comparison between multiple groups was accomplished using either one-way ANOVA followed by Tukey *post hoc* analysis or two-way ANOVA followed by all-pairwise comparison by Student-Newman-Keuls method to compare differences between EtOH and undernutrition. P values ≤ 0.05 were considered statistically significant.

Results

Pregnancy-Induced Changes in EtOH Metabolism. Ethanol metabolism was indirectly estimated *via* monitoring 24 hour UECs in nonpregnant and pregnant

Table 2. Effect of Caloric Intake and Pregnancy on Urine Ethanol Concentrations

Caloric intake (kcal/kg$^{3/4}$/day)	No. of rats	Condition[a]	Peak EtOH concentration (mg/dl)	Nadir EtOH concentration (mg/dl)	Mean UEC (mg/dl)	Integrated area (AUC-UEC)[b]
220	4	Cycling	200 ± 21[c]	29 ± 8[d]	114 ± 15[c]	1253 ± 283[c]
160	4	Cycling	369 ± 25[d]	36 ± 8[d]	202 ± 14[d]	2647 ± 164[d]
220	5	Pregnant	76 ± 8[e]	0[c]	37 ± 4[e]	309 ± 16[e]
160	4	Pregnant	325 ± 53[d]	33 ± 8[d]	179 ± 30[d]	1392 ± 283[c]

[a] Data are from urine collected on days 3–15 of infusion of cycling females or corresponding period in time-impregnated females where infusion (control or 13 g/kg/day of EtOH) began on GD5, as described in Materials and Methods, Study 1.
[b] Represents integrated area under the UEC-days of infusion curve calculated using the trapezoidal rule (Sigmaplot, SPSS). Data represent means ± SEM. Means with differing superscripts are statistically different at a level of $P \leq 0.05$.

dams infused EtOH diets (13 g/kg/day) at two levels of caloric intake (220 kcal/day/kg$^{3/4}$ and 160 kcal/day/kg$^{3/4}$, hereafter referred to as the 220 group and the 160 group, respectively). Mean UECs were approximately 70% lower in the pregnant dams receiving EtOH in the 220 group compared to the nonpregnant counterparts, consistent with previously reported increased EtOH metabolism and clearance in pregnancy (Table 2) (13). However, UECs did not differ statistically between pregnant and nonpregnant rats receiving EtOH in the 160 group, suggesting decreased rate of EtOH metabolism in undernourished pregnant dams. Integrated area under UEC curves (AUC-UEC) were calculated as an estimate of EtOH exposure over the entire experiment. In rats administered ethanol in the 220 group, the AUC-UEC was 75% lower in the pregnant rats compared to nonpregnant dams, consistent with mean UEC estimates (Table 2). While undernutrition led to significantly higher AUC-UEC both in cycling and pregnant dams, indicating higher total EtOH burden, the AUC-UEC in pregnant rats in the 160 group was 50% lower than nonpregnant 160 cohorts, indicating a significant pregnancy-induced increase in EtOH clearance even in the face of undernutrition.

Dose-Response of EtOH Fetal Toxicity. To examine the dose response of EtOH-induced fetal toxicity in rats fed NRC-recommended nutrient levels, various fetal parameters affected by EtOH were recorded (Table 3). UEC levels positively correlated with EtOH dose (Pearson coefficient $r^2 = 0.952$, $P = 0.0009$). Fetal toxicity, as indicated by reduced litter weight and pup birth weight, was only evident at EtOH doses exceeding 11.8 g/kg/day where the mean UECs were greater than 169 ± 15 mg/dl. Although whole litter resorptions were observed at >11.8 g/kg ethanol, complete litter resorptions only reached statistical significance at the 14 g/kg/day dose with average UECs > 300 mg/dl (Table 3). The importance of nutrition to fetal development was seen when we compared rats fed 220 or 160 kcal/kg/day in a separate experiment (Table 4) and found that 63% of dams in the 160 group resorbed their litters at 13 g/kg, whereas none were resorbed in the 220 group. This greater fetal toxicity was associated with a body weight loss (220-EtOH starting body weight 250 ± 5 g and ending body weight 290 ± 9 g vs. 160-EtOH starting body weight 254 ± 4 g and ending body weight 207 ± 7 g, $P \leq 0.05$) throughout gestation and higher mean UECs (Table 4) and AUC-UEC and compared to dams in the 220 group.

Table 3. Effect of Increasing Ethanol Dose on Maternal and Fetal Parameters in Rats Fed 220 kcal/kg$^{3/4}$/day[a]

Ethanol dose (mg/kg/day)	Urine ethanol concentration (mg/dl)	No. of rats	Weight gain (g/day)	% resorption	Pups/litter	Fetal weight (g)	Litter weight (g)
0	0*,**,***	9	8 ± 1.9	0	11 ± 1	3.7 ± 0.3	40 ± 4.4
8	44 ± 4*,**,***	3	8 ± 2.4	0	12 ± 1	3.3 ± 0.2	40 ± 1.8
9	69 ± 6*,**,***	9	8.9 ± 1.6	0	12 ± 1	3.9 ± 0.3	46 ± 2.6
10	118 ± 16*,**	12	9.2 ± 1.8	0	12 ± 1	3.6 ± 0.2	43 ± 4.2
10.75	116 ± 16*,**	9	9.7 ± 1.6	0	12 ± 1	3.6 ± 0.2	45 ± 3.3
11.8	169 ± 15*	9	9 ± 1.7	11	12 ± 1	3.8 ± 0.2	45 ± 4
13	199 ± 16*	15	6.9 ± 1.5	7	12 ± 1	2.3 ± 0.3[b]	27 ± 0.3[b]
14	327 ± 22	3	3.6 ± 1.6[b]	33[b]	4 ± 1[b]	1.4 ± 0.2[b]	6 ± 0.5[b]

[a] Data were collected from time-impregnated females infused from GD5 through GD20 as described in Materials and Methods, Study 2. Data represent means ± SEM. % resorption, % of litters undergoing whole litter resorptions. Pearson product moment correlation analysis between UEC values and average fetal weights shows significant correlation ($r^2 = -0.841$, $P = 0.017$) between the variables.
[b] Significantly different from control (0 mg/kg/day EtOH).
* $P < 0.05$ *versus* 14 g EtOH/kg/day; ** $P < 0.05$ *versus* 13 g EtOH/kg/day; *** $P < 0.05$ *versus* 11.8 g EtOH/kg/day group using one-way ANOVA followed by Tukey *post hoc* analysis.

Table 4. Effect of Undernutrition on Fetal Alcohol Toxicity[a]

Caloric intake (kcal/kg$^{3/4}$/day)	EtOH dose (g/kg/day)	Urine ethanol concentration (mg/dl)	No. of rats	Weight gain (g/day)	% resorption	Pups/litter	Fetal weight (g)	Litter weight (g)
220	13	157 ± 20	7	5.2 ± 1.8	0	12 ± 1	1.9 ± 0.1	22.4 ± 1.7
160	13	233 ± 34[b]	8	−0.9 ± 2.3[b]	63[b]	9 ± 2	1.5 ± 0.2[b]	14.2 ± 2.7[b]

[a] Data were collected from time-impregnated females infused from GD5 through GD20 as described in Materials and Methods, Study 3. Data represent means ± SEM. % resorption, % of litters undergoing full litter resorptions.
[b] Significantly different at $P < 0.05$.

UECs correlated positively with BECs at GD15 ($r^2 = 0.94$). Both parameters, UECs and BECs, showed ~30% higher EtOH levels in the undernourished dams compared to optimally fed cohorts (Fig. 1A). Consistent with maternal EtOH levels, fetal serum and amniotic fluid EtOH concentrations were also higher (~30%) in EtOH-undernourished dams compared to optimally fed counterparts (Fig. 1A). Moreover, undernourished pregnant dams also had greater fetal toxicity as indicated by reduced pup numbers, full litter resorptions, and reduced birth weight ($P \leq 0.05$) (Table 4).

Nutritional Status and Hepatic Alcohol Dehydrogenase mRNA, Protein, and Activity. In order to understand the underlying mechanisms of how undernutrition impairs EtOH metabolism, we examined hepatic EtOH metabolizing enzymes. Activities of hepatic ADH-1 and ALDH were measured in liver homogenates from pregnant dams as described in Study 3 in Materials and Methods. Activity of liver ADH-1 was ~50% lower in 160 group compared to the 220 group (Fig. 1B). In concordance with these data, the mean AUC-UEC was greater in the undernourished pregnant dams ($P \leq 0.05$), indicating reduced EtOH metabolism. ALDH activities (ALDH nmol/mg/min) did not differ significantly between the 160 and 220 groups (1.3 ± 0.3 in EtOH-220 vs. 0.9 ± 0.3 in EtOH-160). Hepatic microsomal CYP2E1 activity (pmol of TBA formed/mg/min) showed a trend towards an increase

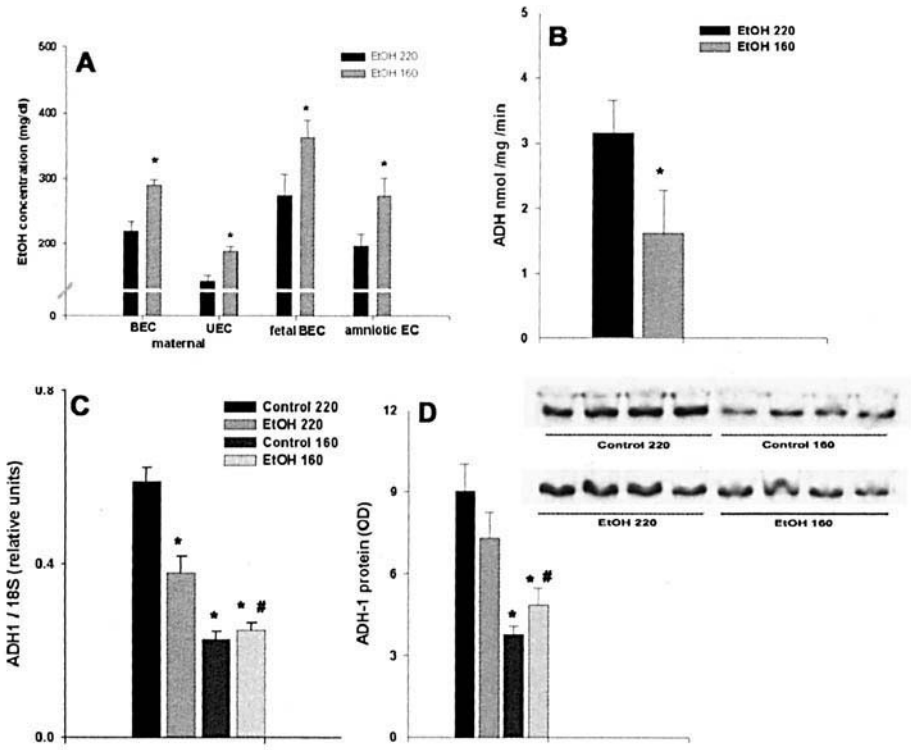

Figure 1. (A) Blood, urine and amniotic fluid ethanol concentrations from pregnant dams and fetal blood ethanol concentrations from dams fed diets containing 12 g of EtOH/kg/day throughout gestation (GD5–GD15) with either 220 kcal/kg$^{3/4}$/day or 160 kcal/kg$^{3/4}$/day (see Materials and Methods, Study 4, for details). Data represent means ± SEM (n=7–8). *, $P < 0.05$ *versus* 220 EtOH group. (B) Hepatic alcohol dehydrogenase activities from pregnant dams fed diets containing 13 g of EtOH/kg/day throughout gestation (GD5–GD15) with either 220 kcal/kg$^{3/4}$/day or 160 kcal/kg$^{3/4}$/day (see Materials and Methods for details). Data represent means ± SEM (n=7–8). *, $P < 0.05$ *versus* 220 EtOH group. (C) Hepatic ADH-1 mRNA. (D) Western blot and densitometric quantitation of ADH-1 protein levels from pregnant dams fed diets containing 12 g of EtOH/kg/day throughout gestation (GD5–GD15) with either 220 kcal/kg$^{3/4}$/day or 160 kcal/kg$^{3/4}$/day (see Materials and Methods, Study 4, for details). Data represent means ± SEM (n=4–9). *, $P < 0.05$ *versus* 220 control group; #, $P < 0.05$ *versus* 220 EtOH group.

Table 5. Ethanol/Nutrition Interaction in Fetal Toxicity Parameters[a]

Diet type and caloric intake (kcal/kg$^{3/4}$/day)	No. of rats	EtOH dose (g/kg/d)	Urine ethanol concentration (mg/dl)	Pups/litter	Litter weight (g)	% resorption
Control- 220	4	0	—	12 ± 0.5	6.5 ± 0.1	0
EtOH-220	8	12	159 ± 18	14 ± 0.3[b]	7.8 ± 0.2[b]	0
Control-160	4	0	—	12 ± 1	6.4 ± 0.7	0
EtOH-160	9	12	254 ± 23[bc]	9.8 ± 2[bcd]	5.2 ± 0.8[bcd]	33[bcd]

[a] Data were collected from time-impregnated females infused from GD5 through GD14 as described in Materials and Methods, Study 4. Data represent means ± SEM. Litter weight, combined weights of the uterus, fetuses, and placenta, as fetuses were too small to be individually weighed. % resorption, % litters undergoing full litter resorptions.
[b] Significantly different from 220 control at same caloric intake.
[c] Significantly different from EtOH 220.
[d] Significantly different from control 220.

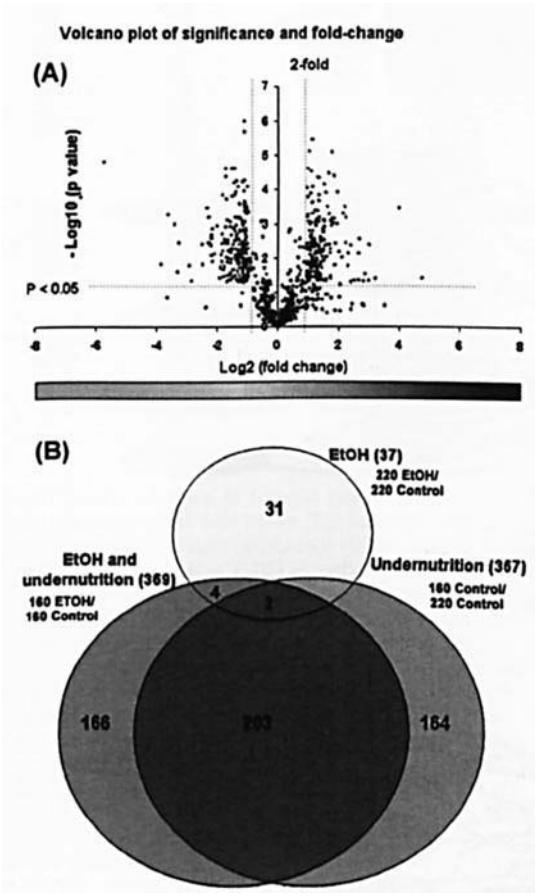

Figure 2. (A) Volcano plot of P value ($-\log_{10}$) versus fold change ($\log_2$) of gene expression data from microarray-based analyses in comparisons of the EtOH 220 (blue) and EtOH 160 (red) groups compared to their respective controls. Genes were filtered based on absence/presence criteria, minimum 2-fold change and $P \leq 0.05$ in either comparison. Four hundred genes passing these criteria are plotted. Genes to the right (or left) and above the vertical and horizontal green lines, respectively, pass the criteria. (B) Venn diagram representation of overall gene expression changes due to EtOH in adequate nutrition (37 genes), EtOH and undernutrition (369 genes), and undernutrition alone (367 genes). Two hundred-three genes were common between undernutrition alone and EtOH combined with undernutrition, revealing 166 unique genes that were affected by EtOH and undernutrition. Data collected from pregnant dams fed diets containing 12 g of EtOH/kg/day throughout gestation (GD5–GD15) with either 220 kcal/kg$^{3/4}$/day or 160 kcal/kg$^{3/4}$/day (see Materials and Methods, Study 4, for details).

in the activity in the undernourished EtOH-fed dams but did not reach statistical significance (86 ± 20 in EtOH-220 vs. 227 ± 88 in EtOH-160).

Furthermore, we examined the decrease in maternal hepatic ADH-1 by measuring gene expression and protein levels. Maternal livers from rats in the 160 or 220 groups receiving control or ethanol diets were used. EtOH-fed 220 dams did not show an induction in ADH-1 compared to controls because the UECs were much below the threshold for ADH-1 induction (>300 mg/dl) (11). Mean mRNA and protein levels of ADH-1 in the 160 group were 50% of those observed in the 220 group ($P < 0.05$, Fig. 1C and D), suggesting that undernutrition may impair EtOH metabolism in pregnancy *via* decreasing hepatic ADH-1.

EtOH-Fetal Toxicity During Maternal Undernutrition. Fetal parameters recorded from pregnant dams fed 12 g/kg/day EtOH from Study 4 confirmed the findings from Study 3. Undernourished EtOH-fed rats showed a marked increase in fetal toxicity parameters, including decreased litter size ($P \leq 0.05$) and complete litter resorptions (33%), compared to none in the 220 EtOH-fed animals (Table 5). Consistent with these data, mean fetal weights at GD20 were significantly lower (1.7 ± 0.04 vs. 1.9 ± 0.04 g, $P < 0.05$) in the EtOH-fed 160 group compared to the controls in the 160 group. Fetal body weights in both the control (2.07 ± 0.07 g) and the EtOH-fed (1.91 ± 0.04) 220 group were also significantly higher ($P < 0.001$) than the 160 EtOH group, but not significantly different from each other. Undernutrition alone in the absence of EtOH did not cause fetal toxicity, suggesting a significant EtOH-nutrition interaction.

Global Maternal Hepatic Gene Expression and EtOH-Undernutrition Interaction. Volcano plot of fold change (±2-fold) of gene expression and P value (≤0.05) shows that ~10-fold greater numbers of genes changed in the maternal livers following EtOH treatment in the 160 group compared to the 220 EtOH group (369 genes vs. 37 genes, respectively, Fig. 2A). The effects of EtOH alone (220 EtOH vs. 220 control), EtOH-undernutrition (160 EtOH vs. 160 control), and undernutrition (160 control vs.

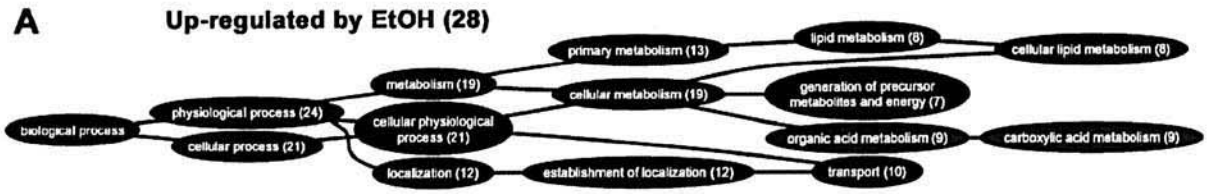
A
Up-regulated by EtOH (28)
primary metabolism (13)
lipid metabolism (8)
cellular lipid metabolism (8)
metabolism (19)
cellular metabolism (19)
generation of precursor metabolites and energy (7)
physiological process (24)
biological process
cellular physiological process (21)
cellular process (21)
organic acid metabolism (9)
carboxylic acid metabolism (9)
localization (12)
establishment of localization (12)
transport (10)

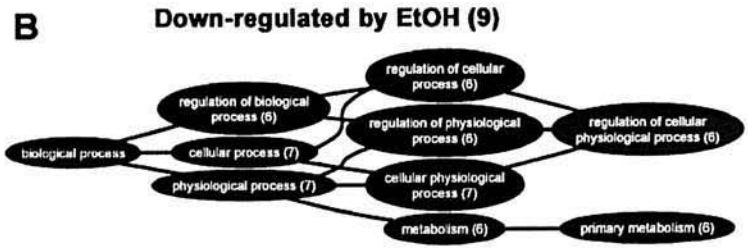
B
Down-regulated by EtOH (9)
regulation of cellular process (6)
regulation of biological process (6)
regulation of physiological process (6)
regulation of cellular physiological process (6)
biological process
cellular process (7)
physiological process (7)
cellular physiological process (7)
metabolism (6)
primary metabolism (6)

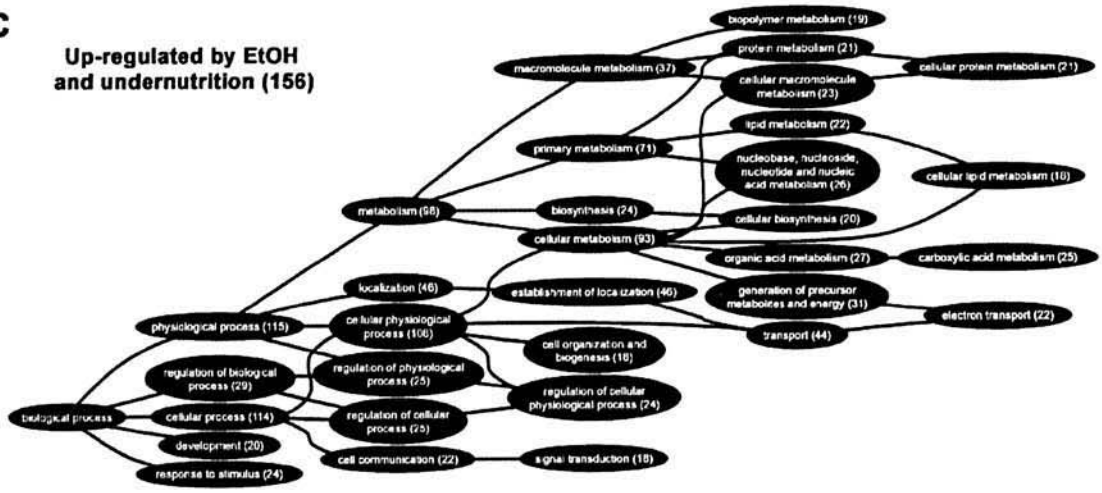
C
Up-regulated by EtOH and undernutrition (156)
biopolymer metabolism (19)
protein metabolism (21)
macromolecule metabolism (37)
cellular protein metabolism (21)
cellular macromolecule metabolism (23)
lipid metabolism (22)
primary metabolism (71)
nucleobase, nucleoside, nucleotide and nucleic acid metabolism (26)
cellular lipid metabolism (10)
metabolism (98)
biosynthesis (24)
cellular biosynthesis (20)
cellular metabolism (93)
organic acid metabolism (27)
carboxylic acid metabolism (25)
localization (46)
establishment of localization (46)
generation of precursor metabolites and energy (31)
electron transport (22)
physiological process (115)
cellular physiological process (106)
transport (44)
cell organization and biogenesis (18)
regulation of biological process (29)
regulation of physiological process (25)
regulation of cellular physiological process (24)
biological process
cellular process (114)
regulation of cellular process (25)
development (20)
cell communication (22)
signal transduction (18)
response to stimulus (24)

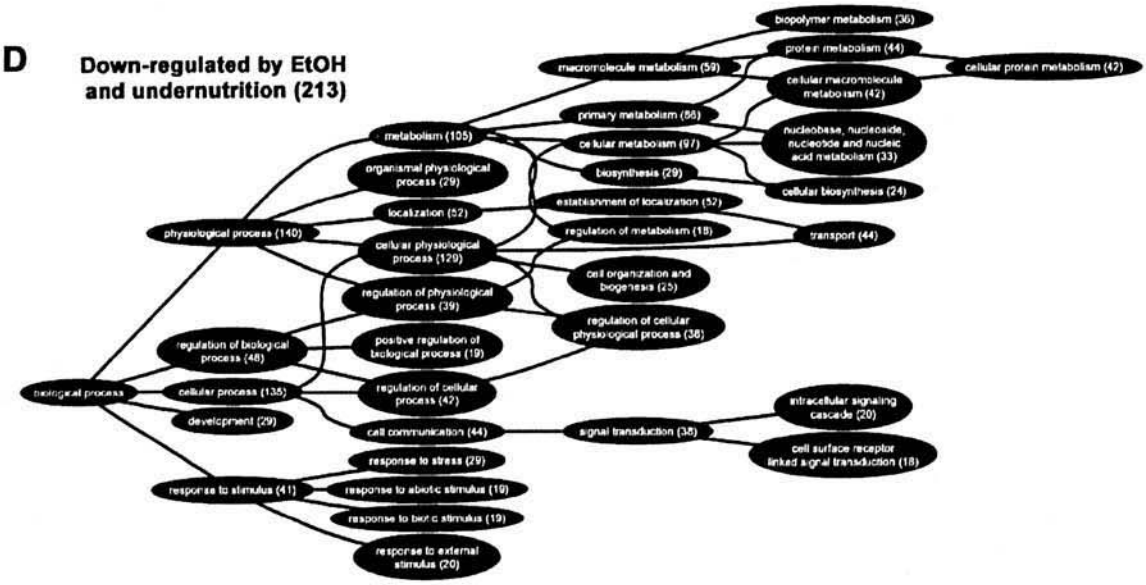
D
Down-regulated by EtOH and undernutrition (213)
biopolymer metabolism (36)
protein metabolism (44)
macromolecule metabolism (59)
cellular protein metabolism (42)
cellular macromolecule metabolism (42)
primary metabolism (86)
metabolism (105)
cellular metabolism (97)
nucleobase, nucleoside, nucleotide and nucleic acid metabolism (33)
organismal physiological process (29)
biosynthesis (29)
cellular biosynthesis (24)
localization (52)
establishment of localization (52)
physiological process (140)
regulation of metabolism (18)
transport (44)
cellular physiological process (129)
cell organization and biogenesis (25)
regulation of physiological process (39)
regulation of cellular physiological process (38)
regulation of biological process (48)
positive regulation of biological process (19)
biological process
cellular process (135)
regulation of cellular process (42)
development (29)
intracellular signaling cascade (20)
cell communication (44)
signal transduction (38)
cell surface receptor linked signal transduction (18)
response to stress (29)
response to stimulus (41)
response to abiotic stimulus (19)
response to biotic stimulus (19)
response to external stimulus (20)

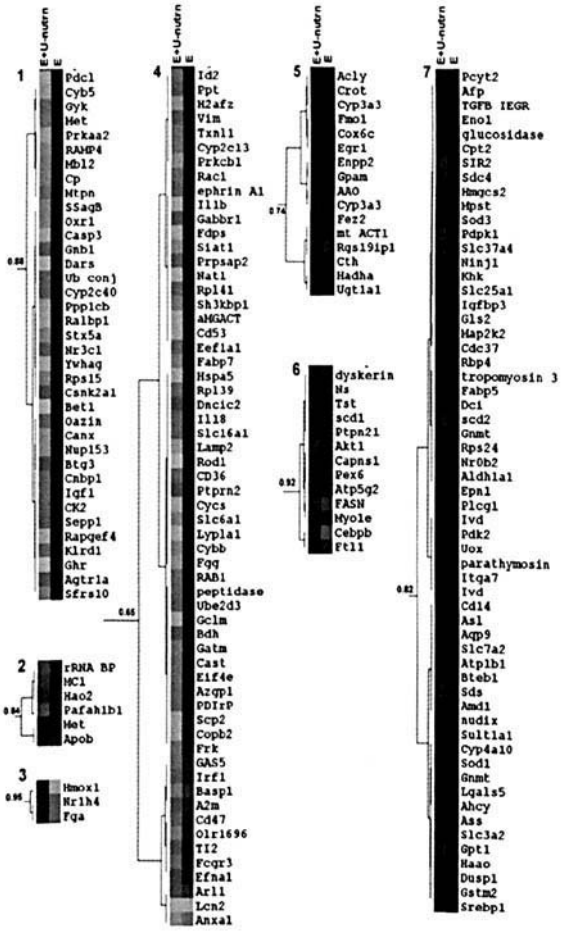

Figure 4. Cluster analysis of hepatic gene expression profiles in EtOH-fed pregnant dams with either 220 kcal/kg$^{3/4}$/day or 160 kcal/kg$^{3/4}$/day. One hundred and ninety-four genes that showed significant change (± 2-fold, $P \leq 0.05$) in either group and had known biological functions (based on annotations from gene ontology biological function, NetAffx, Affymetrix) were selected. Correlation-based hierarchical clustering was performed using Cluster software and data presentation done using Treeview. The gene expression analysis was carried out as described in Materials and Methods. The values represent fold change of each gene transcript in the EtOH-fed group compared to the respective control at the same caloric intake. Gene expression changes are depicted as intensity of color, increase (red), decrease (green), and no change (black). The left columns of the heat map (E + U-nutrn) represent EtOH-induced changes in undernutrition, while the right column (E) represents changes due to EtOH in the adequately fed dams. The dendrogram on the left of the cluster shows relatedness of gene expression change, shorter branches representing closer relationship between gene expression changes. Genes were resolved into seven clusters, with cluster numbers given on the top left side of the cluster diagram based on their gene expression changes. Correlations of their changes are given on the left of the dendrogram.

220 control) are summarized in the Venn diagram (Fig. 2B). Undernutrition by itself altered 367 genes (160 control vs. 220 control). Of those genes altered by undernutrition, 164 genes are not affected by EtOH in the undernourished state. On the other hand, 203 genes that are affected by undernutrition alone are also affected by EtOH during undernutrition (Fig. 2B). Of the genes altered by the combination of EtOH and undernutrition, almost 44% (166 out of 369) are unique changes only represented in the EtOH-undernutrition interaction (160 EtOH vs. 160 control).

Known biological functions of genes were queried and acquired from Affymetrix online data analysis resource NetAffx (http://www.affymetrix.com/analysis/index.affx) and gene ontology analyses performed using GO Browser (Affymetrix). Genes belonging to cellular metabolism, response to stress and stimulus, protein, carbohydrate and lipid metabolism, regulators of cell-cycle and DNA transcription, cell communication and development, and morphogenesis were uniquely changed in the 160 EtOH (EtOH and undernutrition) group (Fig. 3A–D).

Correlation-based hierarchical clustering of 194 genes with known biological functions resolved the affected genes into 7 clusters (Fig. 4, clusters numbered 1 through 7). Correlation coefficients of changes are given on the left of the dendrogram. Complete gene names can be found in Table 6 or queried on NetAffx (http://www.affymetrix.com/analysis/index.affx). Genes in clusters 1, 4, and 7 were significantly changed (decreased in 1 and 4 and increased in 7) uniquely in the EtOH 160 group, while remaining unchanged in the EtOH 220 group. On the other hand, all genes in clusters 3 and 5, and some genes in cluster 6, were changed uniquely by EtOH alone and not affected by the EtOH plus undernutrition. Genes in cluster 2 show a distinct reversal of expression profile in the EtOH 220 and 160 groups.

A more detailed classification of gene expression changes as based on known biological functions is represented in Table 6 and discussed below.

Apoptosis and Cell Proliferation. EtOH combined with undernutrition appeared to shift the status toward a proapoptotic and antiproliferative state. Transforming growth factor-β inducible early growth response, a primary response for TGF-β, mimics TGF-β and regulates differentiation and proliferation and induces apoptosis in many cell types. Proliferative signals such as interleukin-18 (IL-18), IGF-1, growth hormone receptor, and fyn-related kinase were significantly decreased in the 160 EtOH group. Further, met protooncogene (receptor for hepatocyte growth factor), IL-1β, and annexin-1 were also decreased in the 160

Figure 3. Gene ontology analysis of mRNA expression changes by (A–B) EtOH alone or (C–D) EtOH and undernutrition compared to their respective controls (see Materials and Methods, Study 4, for details). Genes were filtered based on absence/presence criteria, minimum 2-fold change and $P \leq 0.05$ in either comparison. Four hundred genes passing these criteria were queried and analyzed using the GO Browser at Affymetrix online data analysis resource NetAffx (http://www.affymetrix.com/analysis/index.affx). Up- and downregulated genes are analyzed separately. Numbers in parentheses denote numbers of genes queried in GO Browser.

Table 6. Microarray Analyses of EtOH and EtOH-Nutrition Interactions[a]

Gene identifier	Gene description	Symbol	EtOH	EtOH and undernutrition
Apoptosis				
rc_AI172476_at	TGFB inducible early growth response	TGFB IEGR	0.95	2.02
U90261UTR#1_g_at	SH3-domain kinase binding protein 1	Sh3kbp1	0.93	−2.44
Cell proliferation and embryonic development				
U77777_s_at	Interleukin 18	Il18	0.98	−2.18
D00698_s_at	Insulin-like growth factor 1	Igf1	1.18	−2.23
Z83757mRNA_g_at	Growth hormone receptor	Ghr	1.41	−4.78
S61868_at	Syndecan 4	Sdc4	0.98	3.56
U72660_at	Ninjurin 1	Ninj1	0.97	2.15
U09583_at	Fyn-related kinase	Frk	1.07	−2.40
rc_AA799542_at	Ras-related C3 botulinum toxin substrate 1	Rac1	0.90	−2.24
rc_AA892598_at	Nucleostemin	Ns	0.71	2.30
U77931_at	rRNA promoter binding protein	rRNA BP	3.09	0.53
X74293_s_at	Integrin alpha 7	Itga7	0.89	2.04
Cell cycle and growth				
M98820_at	Interleukin 1 beta	Il1b	0.87	−3.17
D30040_at	v-akt oncogene homolog 1	Akt1	0.71	5.03
Z46374cds_s_at	Met proto-oncogene	Met	2.40	0.85
rc_AI171962_s_at	Annexin A1	Anxa1	−2.30	−2.78
D26564_g_at	Cell division cycle 37	Cdc37	1.02	2.01
rc_AI009405_s_at	Insulin-like growth factor binding protein 3	Igfbp3	0.96	3.39
rc_AA875506_at	Casein kinase II, alpha 1 polypeptide	Csnk2a1	1.29	−2.04
M57276_at	CD53 antigen	Cd53	0.91	−2.98
L24776_at	Tropomyosin 3, gamma	tropomyosin 3	1.13	2.65
rc_AI137583_at	Inhibitor of DNA binding 2	Id2	0.80	−2.19
Regulators of DNA transcription				
D12769_at	Basic transcription element binding protein 1	Bteb1	1.58	2.91
D44494_at	3-hydroxyanthranilate 3,4-dioxygenase	Haao	1.21	2.55
D86745cds_s_at	Nuclear receptor subfamily 0, group B, member 2	Nr0b2	1.07	2.35
M14053_at	Nuclear receptor subfamily 3, group C, member 1	Nr3c1	1.29	−2.13
rc_AI105463_at	Myotrophin	Mtpn	1.61	−2.28
rc_AA859536_at	Brain abundant signal protein 1	Basp1	0.58	−2.48
S77528cds_s_at	CCAAT/enhancer binding protein β	Cebpb	0.51	2.80
U18374_at	Nuclear receptor subfamily 1, group H, member 4	Nr1h4	−2.11	0.84
D45254_g_at	Cellular nucleic acid binding protein 1	Cnbp1	1.19	−2.23
J05499_at	Glutaminase 2 (liver, mitochondrial)	Gls2	1.00	2.75
M34253_g_at	Interferon regulatory factor 1	Irf1	0.67	−2.12
M18416_at	Early growth response 1	Egr1	2.79	2.68
L16995_at	Sterol regulatory element binding protein 1	Srebp1	1.16	2.49
Glucose metabolism				
J03863_at	Serine dehydratase	Sds	4.09	27.29
S69874_s_at	Fatty acid binding protein 5, epidermal	Fabp5	1.12	2.54
rc_AA892486_at	α-glucosidase	glucosidase	0.96	1.96
AF080468_g_at	Solute carrier family 37	Slc37a4	0.97	3.55
X02610_at	Enolase 1, alpha	Eno1	0.95	2.86
M86235_at	Ketohexokinase	Khk	0.96	2.60
AB015433_s_at	Solute carrier family 3	Slc3a2	1.20	2.46
D16102_at	Glycerol kinase	Gyk	1.89	−2.23
Lipid and fatty acid biosynthesis and metabolism				
AF036761_g_at	Stearoyl-Coenzyme A desaturase 2	scd2	1.24	8.01
J02585_at	Stearoyl-Coenzyme A desaturase 1	scd1	0.71	2.67
M76767_s_at	Fatty acid synthase	FASN	0.59	6.40
D00729_g_at	Dodecenoyl-coenzyme A delta isomerase	Dci	1.10	2.68
X98225_s_at	Hydroxyacyl-Coenzyme A dehydrogenase	Hadha	1.98	1.39
U36772_at	Glycerol-3-phosphate acyltransferase, mitochondrial	Gpam	1.84	2.30
J05470_at	Carnitine palmitoyltransferase 2	Cpt2	0.98	2.47
rc_AA925752_at	cd36 antigen	CD36	1.03	−2.22
Y09333_at	MT acyl-CoA thioesterase 1	mt ACT1	3.35	1.54
U97146_at	Lysophospholipase 1	Lypla1	1.07	−3.58
L27075_g_at	ATP citrate lyase	Acly	2.43	1.82

Table 6. (Continued)

Gene identifier	Gene description	Symbol	EtOH	EtOH and undernutrition
U10357_at	Pyruvate dehydrogenase kinase 2	Pdk2	0.90	2.66
M33648_at	3-hydroxy-3-methylglutaryl-Coenzyme A synthase 2	Hmgcs2	0.99	1.97
M58287_s_at	Sterol carrier protein 2	Scp2	1.14	−3.61
U53873cds_at	Apolipoprotein B	Apob	4.03	0.84
Electron transport				
J05031_at	Isovaleryl coenzyme A dehydrogenase	Ivd	0.87	3.07
X07259cds_s_at	Cytochrome P450 4A10	Cyp4a10	1.35	2.56
M27467_at	Cytochrome c oxidase VIc	Cox6c	2.30	1.98
X62086mRNA_s_at	Cytochrome P450 3A3	Cyp3a3	2.59	1.98
J03786_s_at	Cytochrome P450 2C40	Cyp2c40	1.30	−2.17
M86870_at	Protein disulfide isomerase related protein	PDIrP	1.08	−2.21
J02861mRNA_s_at	Cytochrome P450 2C13	Cyp2c13	0.84	−2.25
rc_AA894029_at	Endothelial type gp91-phox gene	Cybb	1.06	−2.53
rc_AA875390_g_at	Thioredoxin-like (32kD)	Txnl1	0.85	−2.23
rc_AA945054_s_at	Cytochrome b-5	Cyb5	2.21	−2.91
L15354_s_at	Phosducin-like	Pdcl	2.39	−3.22
rc_AI232087_at	Hydroxyacid oxidase 2	Hao2	2.26	0.66
rc_AI008815_s_at	Cytochrome c	Cycs	1.02	−3.18
M84719_at	Flavin monooxygenase 1	Fmo1	3.17	2.78
AB003400_at	D-amino acid oxidase	AAO	2.02	2.83
Stress and stimuli response				
rc_AI233261_i_at	Glutamate cysteine ligase	Gclm	1.19	−3.42
rc_AA900582_at	Alpha-2-macroglobulin	A2m	0.65	−2.06
M22993cds_s_at	Murinoglobulin 1	MC1	2.64	0.60
J00735_at	Gamma fibrinogen	Fgg	1.05	−2.81
AF087943_s_at	CD14 antigen	Cd14	1.74	3.32
rc_AI112173_at	Na^+/K^+ ATPase beta 1	Atp1b1	1.34	1.95
rc_H33461_at	Oxidation resistance 1	Oxr1	1.49	−2.52
D49708_at	Arginine/serine-rich splicing factor	Sfrs10	1.19	−2.45
Z24721_at	Superoxide dismutase 3	Sod3	0.98	2.13
rc_AA875089_at	Calpastatin	Cast	1.15	−2.29
rc_AA893328_at	Calnexin	Canx	1.28	−2.78
S63521_i_at	Heat shock 70kD	Hspa5	1.00	−3.27
L34262_at	Palmitoyl-protein thioesterase	Ppt	0.83	−2.05
U13177_at	Ubiquitin-conjugating enzyme	Ube2d3	1.11	−2.14
U53859_g_at	Calpain, small subunit 1	Capns1	0.83	2.52
D13907_g_at	Peptidase, beta	peptidase	1.11	−2.25
J02592_s_at	Glutathione S-transferase, mu 2	Gstm2	1.14	2.17
Protein biosynthesis and metabolism				
rc_AA819643_at	AMP-activated protein kinase, alpha 2	Prkaa2	1.82	−2.92
rc_AA963674_g_at	Mitogen activated protein kinase kinase 2	Map2k2	1.00	2.05
X04139_s_at	Protein kinase C, beta 1	Prkcb1	0.79	−2.74
U78517_at	cAMP-regulated guanine nucleotide exchange factor II	Rapgef4	1.30	−3.31
Y15748_at	3-phosphoinositide dependent protein kinase-1	Pdpk1	0.92	15.97
U02553cds_s_at	Dual specificity phosphatase 1	Dusp1	1.29	3.30
U17971_at	Protein tyrosine phosphatase 2E	Ptpn21	0.70	2.54
AF100470_at	Ribosome associated membrane protein 4	RAMP4	1.70	−2.65
M83143_g_at	Sialyltransferase 1	Siat1	0.86	−2.66
rc_AI171085_at	Ribosomal protein L39	Rpl39	0.99	−2.24
M89646_at	Ribosomal protein S24	Rps24	1.05	2.19
rc_AA892895_i_at	Ribosomal protein S15	Rps15	1.35	−2.51
AA944073_at	Ribosomal protein L41	Rpl41	0.96	−2.16
M81088_at	Eukaryotic translation elongation factor 1 alpha 1	Eef1a1	0.93	−2.17
X83399_at	Eukaryotic translation initiation factor 4E	Eif4e	1.08	−2.30
rc_AI009682_s_at	Aspartyl-tRNA synthetase	Dars	1.98	−4.30
Intracellular transport				
K03045cds_r_at	Retinol binding protein 4, plasma	Rbp4	1.12	2.56
U02096_at	Fatty acid binding protein 7, brain	Fabp7	1.00	−2.47
rc_AA818240_at	Nucleoporin 153kD	Nup153	1.34	−2.75
U53927_at	Solute carrier family 7, member 2	Slc7a2	1.40	2.19

Table 6. (Continued)

Gene identifier	Gene description	Symbol	EtOH	EtOH and undernutrition
rc_AA946503_at	Lipocalin 2	Lcn2	−5.18	−7.12
U75400_s_at	Coatomer protein complex, subunit beta 2	Copb2	1.10	−3.29
U42755_at	Blocked early in transport 1 homolog	Bet1	1.47	−4.53
U87971_at	Syntaxin 5a	Stx5a	1.38	−2.64
rc_AA817854_s_at	Ceruloplasmin	Cp	1.75	−2.54
L12016_at	Solute carrier family 25, member 1	Slc25a1	0.97	2.52
U82623_at	ralA binding protein 1	Ralbp1	1.47	−3.18
rc_AI228669_at	GABA transporter protein	Slc6a1	1.01	−2.53
D63834_at	Solute carrier family 16, member 1	Slc16a1	0.98	−2.17

[a] Data were collected from time-impregnated females ($N=3$) infused from GD5 through GD15 as described in Materials and Methods, Study 4. Hepatic gene expression profiles were assessed using Affymetrix RGU34A GeneChip microarrays according to manufacturer's instructions. EtOH column represents ratios of mean gene expression of EtOH 220 group compared to control 220. EtOH and undernutrition column represents ratios of mean gene expression of EtOH 160 compared to control 160 group. All ratios showing ±2-fold change are also significantly different ($P \leq 0.05$) using Student's t test.

EtOH group. Casein kinase 2, a ubiquitous and highly conserved serine/threonine kinase with important roles in cell growth, proliferation, and suppression of apoptosis, was also decreased in the EtOH 160 group (Table 6).

Regulators of DNA Transcription. Nutrient sensing transcription factors 3-hydroxyanthrinilate 3,4-dioxygenase (involved in tryptophan metabolism), CAAT-enhancer binding protein-β (C/EBP β, glucose signaling), and sterol-regulatory element binding protein-1 (SREBP-1, fatty acid biosynthesis) were increased in the 160 EtOH group. The Kruppel-like family member, basic transcription element binding protein (BTEB-1), that regulates expression of pregnancy associated genes was increased in the EtOH 160 group. Nuclear receptor Nr3c1 (glucocorticoid receptor) was decreased specifically in the 160 EtOH group, suggesting changes in glucocorticoid signaling. The stress response transcription factor, early growth response 1, was induced equally in both the 220 and 160 EtOH groups (Table 6).

Lipid and Glucose Metabolism. Undernutrition resulted in a robust increase in gluconeogenic genes. EtOH combined with undernutrition further induced liver serine dehydratase mRNA to 27-fold, compared to the 4-fold induction by EtOH alone. Gene expression of ketohexokinase, slc37a4 (glucose 6-phosphate translocase), and enolase 1 was significantly increased in the EtOH 160 group, indicating increased gluconeogenesis. Genes responsible for biosynthesis of triglycerides (scd1, scd2, FASN) were induced in the EtOH 160 group compared to the 160 controls, suggesting that the acetate generated from the oxidation of EtOH was shunted into fatty acid biosynthesis (Table 6).

Electron Transport and Stress Response. The majority of genes belonging to electron transport were decreased in the EtOH 160 group, while either remaining unchanged or increased in the EtOH 220 group. The rate-limiting step in glutathione biosynthesis, glutamate cysteine ligase, was decreased 3-fold in the 160 EtOH group. Several genes involved in mediating cellular stress response, including hsp70, calpastatin, calnexin, oxidation resistance 1, ubiquitin-conjugating enzyme, and α2-macroglobin, were decreased in the EtOH 160 group (Table 6).

Protein Transcription and Intracellular Transport. Gene expression of critical kinases such as c-AMP activated protein kinase (AMPK), protein kinase C (PKC), and cAMP regulated nucleotide exchange factor were decreased, accompanied by increases in gene expression of the protein phosphatases Dusp1 and Ptpn21. Significant decreases in mRNAs for at least 8 different factors associated with ribosomal protein synthesis and translation were observed. Genes associated with intracellular transport such as Fabp7, Bet1, Slc25a1 (mitochondrial carrier), Slc16a1 (monocarboxylate transporters), Slc6a1 (GABA transporter), syntaxin-5a, and ralA binding protein were uniquely downregulated in the EtOH 160 group (Table 6).

Gene expression of several genes observed in the microarray analyses were confirmed *via* real-time RT-PCR analyses (Table 7). Linear regression analysis of fold changes of 14 genes (Table 7, Fig. 6C and D) obtained *via* real-time RT-PCR compared to microarray-based gene expression analyses revealed highly significant positive correlation ($P < 0.001$, $r^2 = 0.59$, slope = 1.073). Among genes used to confirm microarray results, several genes (rPER2, glucK, PEPCK, PrlR, MT1, rev-erbA-α, and rev-erbA-β) altered in the EtOH 160 group, compared to the control 220 group, were mainly due to the undernutrition effect (Table 7). In contrast, metallothionein 2 (MT2) mRNA expression was increased (~190%) in the EtOH 160 group compared to the 160 control, revealing a significant EtOH-undernutrition interaction.

The resulting set of 194 genes from microarray analyses with known biological functions (Table 6) was further analyzed using PathwayAssist software (Ariadne Genomics) to identify relationship of genes and known signaling pathways using curated databases. Of the 194 genes queried, 84 genes showed connectivity to other known genes. The top three genes (showing maximum connectivity) were AKT1 (a

Table 7. Real-time RT-PCR Analyses of EtOH and EtOH-Nutrition Interactions[a]

	Control-220		EtOH-220		Control-160		EtOH-160	
Gene name	Microarray	Real-time RT-PCR	Microarray	Real-time RT-PCR	Microarray	Real-time RT-PCR	Microarray	Real-time RT-PCR
Glucokinase (glucK)	1 ± 0.33	1 ± 0.2	0.6 ± 0.07	0.74 ± 0.1[b]	0.19 ± .01	0.14 ± 0.04[c]	0.15 ± 0.03	0.25 ± 0.08
Phosphoenolpyruvate carboxykinase (PEPCK)	1 ± 0.5	1 ± 0.2	2.6 ± 0.9	1.78 ± 0.3[b]	4.03 ± 0.8	3.47 ± 1.03[c]	4.9 ± 1.14	3.86 ± 1.6
Mitochondrial cytochrome B (MT cytB)	1 ± 0.06	1 ± 0.05	0.65 ± 0.2	0.92 ± 0.05	0.49 ± 0.2	0.89 ± 0.02	0.89 ± 0.17	0.86 ± 0.02
Prolactin receptor (PrlR)	1 ± 0.05	1 ± 0.07	1.43 ± 0.08	1.50 ± 0.03	1.89 ± 0.38	2.33 ± 0.3[c]	1.4 ± 0.25	2.20 ± 0.4
CD36 antigen (CD36)	1 ± 0.08	1 ± 0.04	1.63 ± 0.07	1.29 ± 0.1	1.76 ± 0.16	1.52 ± 0.1	0.81 ± 0.25	1.30 ± 0.2
Metallothionein 1 (MT1)	1 ± 0.71	1 ± 0.1	1.59 ± 0.51	1.81 ± 0.2[b]	12 ± 2.9	4.90 ± 0.3[c]	19.9 ± 0.7	6.70 ± 0.9
Metallothionein 2 (MT2)	1 ± 0.38	1 ± 0.2	1.44 ± 0.38	1.59 ± 0.5	6.08 ± 0.2	3.32 ± 0.3[c]	8.59 ± 0.5	6.29 ± 0.3[b]
Rev-erbA alpha (rev-erbAα)	1 ± 0.25	1 ± 0.4	1.3 ± 0.37	1.41 ± 0.5	3.4 ± 1.5	12.92 ± 3.0[c]	26 ± 7.7	19.15 ± 0.4
Rev-erbA beta (rev-erbAβ)	1 ± 0.35	1 ± 0.1	1.5 ± 0.61	1.61 ± 0.2	7.9 ± 1.09	5.37 ± 0.9[c]	9.9 ± 2.42	5.37 ± 0.30
Period (rPER2)	1 ± 0.16	1 ± 0.03	0.7 ± 0.17	0.59 ± 0.2	0.08 ± 0.02	0.15 ± 0.02[c]	0.12 ± 0.07	0.18 ± 0.005
Fas ligand (FASL)	1 ± 0.12	1 ± 0.3	2.39 ± 0.84	0.83 ± 0.2	2.1 ± 0.95	0.68 ± 0.1	1.7 ± 0.35	1.13 ± 0.6
Cyclooxygenase 1 (COX1)		1 ± 0.04		1.17 ± 0.07		1.09 ± 0.09		1.40 ± 0.06
18 S rRNA (18S)		1 ± 0.09		0.96 ± 0.04		0.98 ± 0.02		1.01 ± 0.002

[a] Data were collected from time-impregnated females infused from GD5 through GD15 as described in Materials and Methods, Study 4. Real-time PCR reactions were carried out according to manufacturer's instructions for 2X SYBR Green master mix and monitored on an ABI Prism 7000 sequence detection system (Applied Biosystems, Foster City, CA) as described in Materials and Methods. Data are expressed as change over the control 220 group. Linear regression analysis of fold changes of 14 genes (Table 7, Fig. 5C and D) obtained *via* real-time RT-PCR compared to microarray-based gene expression analyses revealed highly significant positive correlation ($P < 0.001$, $r^2 = 0.59$, slope = 1.073).

[b] Significantly different from control at same caloric intake.

[c] Significantly different from 220-control.

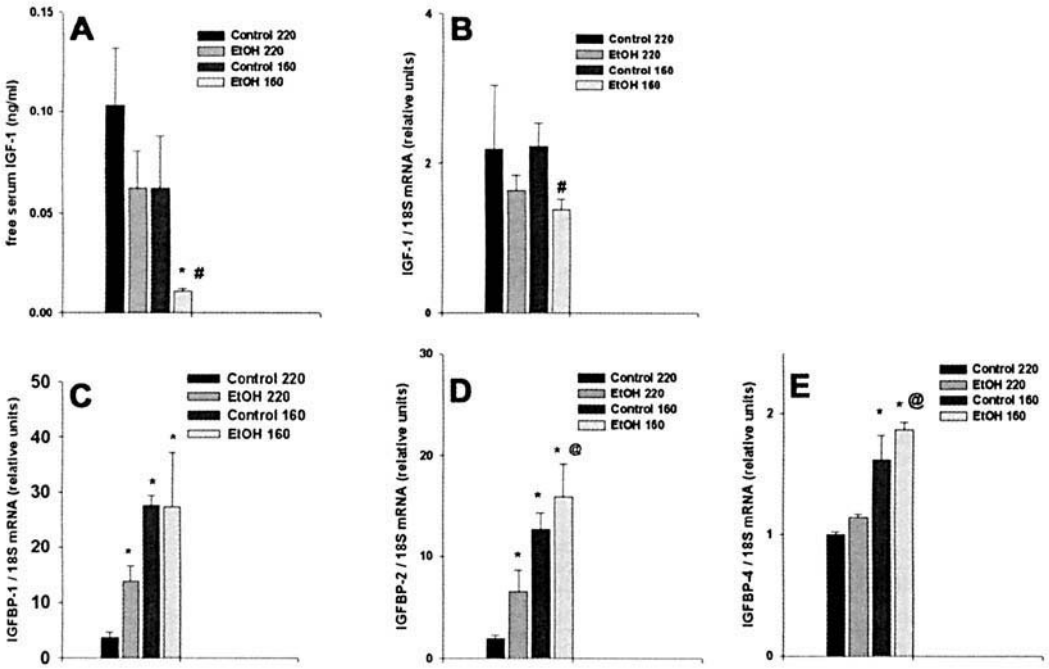

Figure 5. Maternal (A) serum-free insulin-like growth factor-1 (IGF-1) protein, (B) hepatic IGF-1, (C) IGFBP-1, (D) IGFBP-2, (E) IGFBP-4 mRNA expression normalized to 18S ribosomal RNA gene expression from pregnant dams fed diets containing 12 g of EtOH/kg/day throughout gestation (GD5–GD15) with either 220 kcal/kg$^{3/4}$/day or 160 kcal/kg$^{3/4}$/day (see Materials and Methods, Study 4, for details). Data represent means ± SEM ($n = 4$–9). *, $P < 0.05$ *versus* 220 control group; #, $P < 0.05$ *versus* 160 control group; @, $P < 0.05$ *versus* 220 EtOH group.

serine theornine kinase), IL-1β (cytokine), and IGF-1 (growth factor), all with greater than 2000 interactions with known proteins and signaling molecules. Since IGF-1 has a bona fide role in fetal growth and development and can itself act as a regulator of AKT-1 and IL-1β, we decided to further examine IGF-1 protein levels and signaling.

IGF-1 Protein and Gene Expression in Undernourished Pregnant Dams Fed EtOH. To further investigate the mechanisms of intrauterine growth retardation we assessed maternal IGF-1 status, thought to be an important regulator of fetal growth (19–21). Consistent with the fetal growth data, serum IGF-1 concentrations were not significantly reduced by EtOH in the 220 group or by undernutrition alone. However, compromised nutrition in combination with EtOH led to a remarkable decrease ($P \leq 0.005$) in free serum IGF-1 concentrations (~90%) compared to control 220 group (Fig. 5A).

Changes in hepatic IGF-1 mRNA levels seen in microarrays were confirmed using *real-time* RT-PCR. Consistent with serum IGF-1 levels, the EtOH-treated 220 group did not have decreased IGF-1 gene expression (Fig. 5B). In contrast, undernourished EtOH-fed animals had 40% lower IGF-1 mRNA level compared to the TEN 160 group ($P \leq 0.05$). Undernutrition alone did not change IGF-1 mRNA levels (Fig. 5B). Expression of 18S ribosomal RNA, assessed as a housekeeping gene, did not change (data not shown).

IGFBP-1, -2 and -4 Gene Expression in Undernourished Pregnant Dams. Consistent with earlier reports, maternal hepatic mRNA of both IGFBP-1 and -2 were increased ~4-fold due to EtOH in the 220 group (Fig. 5C and D). Undernutrition markedly induced IGFBP-1 and -2 gene expression to almost 6- to 9-fold higher than the 220 group (Fig. 5C and D). A more modest (~1.8-fold) but significant ($P \leq 0.05$) increase was observed in IGFBP-4 mRNA both in the control and EtOH-fed undernourished dams (Fig. 5E).

EtOH-Undernutrition and STAT5a and -5b Signaling. IGF-1 synthesis is known to be controlled in a growth hormone–dependent manner. Recent evidence suggests that both STAT5a and STAT5b are critical for IGF-1 gene expression (22). Since undernourished pregnant dams fed EtOH had lower IGF-1 gene expression, we examined the status of hepatic STAT5a and-5b (Fig. 6A and B). Western blot analyses revealed that EtOH-fed undernourished dams had ~75% lower levels ($P \leq 0.05$) of STAT5a compared to control 220 group. Undernutrition by itself (without EtOH) also decreased STAT5a levels ($P \leq 0.05$). Pregnant dams fed EtOH in the 220 group did not have significant decreases in STAT5a levels. Modulation of STAT5b levels was similar to that of STAT5a. Undernourished EtOH-fed rats produced lower levels of STAT5b compared to the 220 groups, with or without ethanol ($P \leq 0.005$). Undernutrition by itself did not significantly change STAT5b levels.

We further investigated whether undernutrition and EtOH affect STAT5a and -5b gene expression. Consistent with protein changes, undernutrition by itself (without

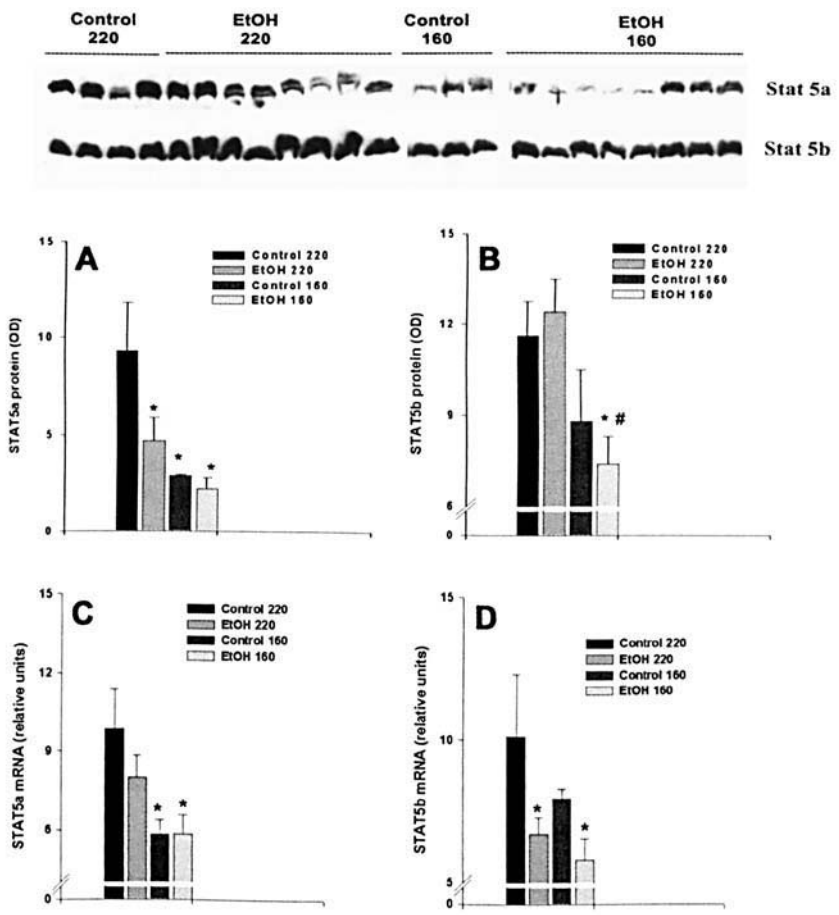

Figure 6. Hepatic (A) STAT5a and (B) STAT5b protein levels, and (C) STAT5a and (D) STAT5b mRNA levels in pregnant dams fed control diets or diets containing 12 g of EtOH/kg/day throughout gestation (GD5–GD15) with either 220 kcal/kg$^{3/4}$/day or 160 kcal/kg$^{3/4}$/day. Data represent means ± SEM (n = 3–8). Top panel shows representative blots. Left and right bottom panels show graphical densitometric quantitation of STAT5a and STAT5b proteins, respectively. *, $P < 0.05$ *versus* 220 control group; #, $P < 0.05$ *versus* 220 EtOH group.

EtOH) decreased STAT5a mRNA levels compared to 220 control ($P \leq 0.05$, Fig. 6C). Undernourished EtOH-fed rats had lower levels of STAT5b mRNA compared to 220 controls ($P \leq 0.05$, Fig. 6D). These data suggest that undernutrition and EtOH produced STAT5 inhibition, which may at least partly be mediated at the transcriptional or the pretranslational level.

IGF and IGFBP Changes in Fetuses from EtOH-Exposed Dams. We measured free serum IGF-1 in GD20 fetuses from dams fed EtOH (12 g/kg/day) in the 220 or 160 groups. Neither the serum IGF-1 protein (Fig. 7A) nor hepatic mRNA for IGF-1 were significantly different in any of the groups, but there was a tendency for suppression of IGF-1 mRNA (Fig. 7B). IGF-2 mRNA was significantly induced by combination of undernutrition and ethanol compared to both the 220 control and ETOH groups (Fig. 7C). Serum IGF-2 protein was not measured, since there is no commercially available rat assay. These findings suggest differential regulation of IGF-1 in maternal versus fetal compartments. IGFBP-1 and -2 mRNA expression was also selectively induced (~2-fold) in the livers of undernourished-EtOH fed fetuses ($P < 0.05$, Fig. 7D and E).

Discussion

Nutrition plays an important role in assuring a normal pregnancy. Although it has been known for years that there is an important interaction between EtOH and nutrient intake during pregnancy and fetal development, the standard rodent models have not been adequate to study the role of maternal nutrition on the detrimental effects of EtOH on the growing fetus. The TEN model provides a unique opportunity to study the effects of nutrition and EtOH separately and in concert with each other. Using the TEN system, we have demonstrated that ethanol-induced fetal growth retardation is potentiated by undernutrition. The present studies examine the mechanisms involved in the interaction of EtOH and nutrition on *in utero* growth effects.

The continuous intragastric EtOH infusion model is characterized by well-defined pulses in BECs and UECs that occur with a frequency of 6–7 days (11). EtOH-dependent induction of hepatic ADH-1 underlies the cyclic behavior of blood and urine EtOH concentrations (23). Upon chronic EtOH infusion, hepatic ADH-1 is transcriptionally induced, in part *via* positive regulation by C/EBP β (LAP isoform) and EtOH-mediated suppression of SREBP-1 (a

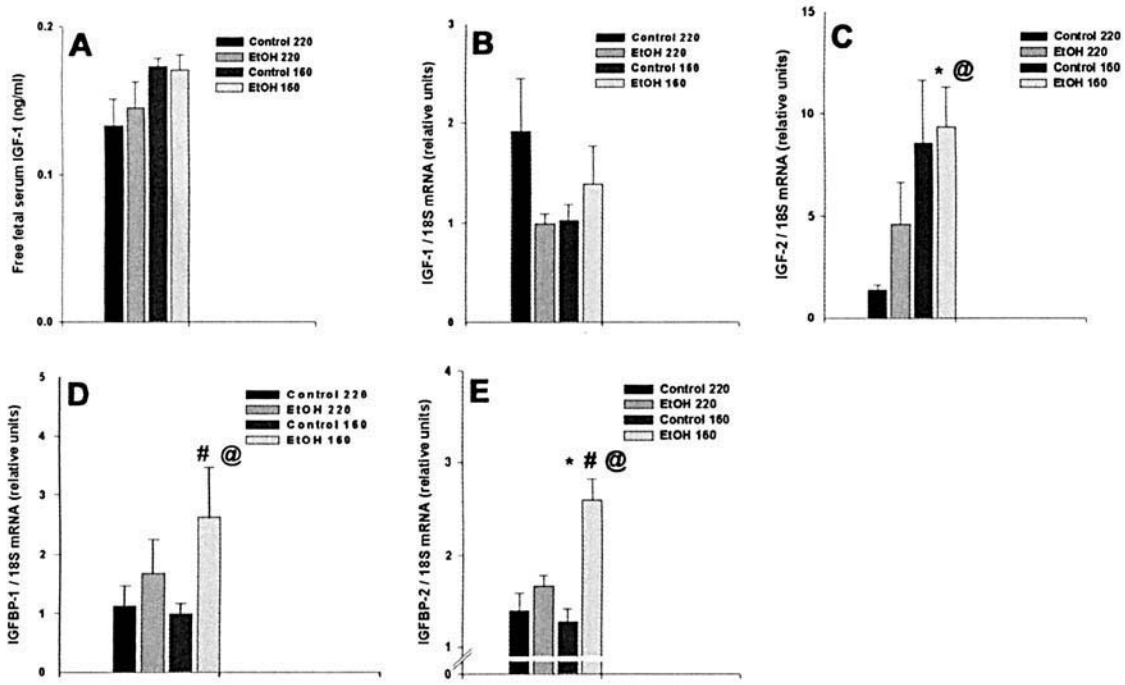

Figure 7. (A) Fetal serum-free IGF-1, (B) fetal hepatic IGF-1, (C) IGF-2, (D) IGFBP-1, and (E) IGFBP-2 mRNA expression in fetuses from pregnant dams fed diets containing 12 g of EtOH/kg/day throughout gestation (GD5–GD20) with either 220 kcal/kg$^{3/4}$/day or 160 kcal/kg$^{3/4}$/day (see Materials and Methods, Study 4, for details). Blood was pooled from all fetuses per dam. Data represent means ± SEM ($n = 4$–9). *, $P <$ 0.05 *versus* 220 control group; #, $P < 0.05$ *versus* 160 control group; @, $P < 0.05$ *versus* 220 EtOH group.

negative regulator of ADH-1 transcription) (16, 24). In the present study, pregnant dams receiving EtOH diets at 220 kcal/kg$^{3/4}$/day did not show an induction in ADH-1 mRNA. The primary reason for the lack of ADH-1 induction may be related to the low UECs (and BECs) attained in the pregnant dams. EtOH-mediated induction of ADH-1 is closely tied to the dose and resultant circulating levels of EtOH. Chronic infusion studies suggest that the threshold for ADH-1 induction is at UECs > 300 mg/dl. Pregnancy enhances whole-body EtOH clearance primarily *via* increased gastric first-pass metabolism in a manner independent of caloric intake (13). Consistent with earlier reports (11, 13), pregnant dams in the present study also showed increased EtOH clearance and UECs below the threshold for ADH-1 induction.

Several possible mechanisms underlying EtOH-nutrient interactions have been explored in our studies. It is clear that EtOH metabolism itself is decreased in the undernourished state, since undernourished dams had greater mean UECs and BECs compared to pregnant rats fed NRC-recommended calories and infused the same EtOH dose (g/kg/day). In addition, impairment of EtOH metabolism directly translated into greater fetal exposure to EtOH, as evidenced by the higher amniotic fluid and blood EtOH concentrations. Hepatic ADH-1, which was significantly lower in the undernourished pregnant EtOH-fed dams, is responsible for about 75%–90% of *in vivo* EtOH metabolism (25, 26). The resulting metabolite, acetaldehyde, is rapidly converted to acetate *via* the ALDH system in the mitochondria. ALDH activities were not affected by undernutrition in pregnancy. Hence, it seems reasonable that the lower rate of EtOH metabolism by ADH-1 in undernutrition significantly increases the potential of fetal toxicity by increasing the EtOH exposure to maternal and fetal tissues. Undernutrition and fasting have previously been shown to decrease ADH-1 activity (27–29). Although the mechanisms of how nutrition modulates ADH-1 levels are not clear, data from the present studies show a decrease of ADH-1 mRNA due to undernutrition. Several hormones, including growth hormone (GH), thyroid hormone, and androgens that affect ADH mRNA levels (30), might be modulated by nutrition. Several transcription factors, including C/EBP β, SREBP-1 (16, 26), and STAT5b (31), have been reported to be regulate ADH-1 transcription. C/EBPs and SREBPs are transcription factors that play important roles in energy metabolism and can be modulated by nutritional status (32). Further, data from our microarray analyses (Table 6, under Regulators of DNA transcription) showed induction of SREBP-1c, a negative ADH-1 regulator, in undernourished EtOH-fed dams. Also, decreased STAT5b levels (a positive regulator of ADH-1) were observed in the undernourished EtOH-fed dams, consistent with lower ADH-1 levels. Hence the hypothesis that undernutrition impairs EtOH metabolism by decreasing ADH-1 levels *via* altered C/EBPs, SREBP-1c, or STAT5b signaling is worthy of further investigation.

To further understand the molecular mechanisms of EtOH-undernutrition interactive toxicity, we utilized microarrays to generate mechanistic leads. Although expression

of a large number of genes was altered, a closer examination of the data revealed that IGF-1 was decreased by EtOH during undernutrition and several genes across different functional families known to be regulated by IGF-1 were also altered, making it a candidate for further investigation. For example, casein kinase activity, which is directly increased with IGF-1, was decreased in correlation with IGF-1 (33). Expression of other IGF-1 regulated genes such as AMPK, MAPKK2, PKC-β, and several members of the ribosomal proteins and translation elongational factors involved in protein synthesis were also decreased. Furthermore, gene expression of the growth hormone receptor and IGFBP-3 was significantly altered so as to decrease IGF-1 signaling.

Several growth factors, including IGF-1, are important in placental and fetal development (19–21). Exposure to EtOH decreases circulating IGF-1 levels in both animal models and humans (34, 35). EtOH also inhibits the autophosphorylation of the IGF-1 receptor (36). In addition, EtOH feeding *via* oral liquid diets to pregnant dams (which also decrease food intake) has been shown to result in ~50% reduction in serum IGF-1 levels (37). These data are consistent with our findings that show ~50% decrease in hepatic IGF-1 mRNA and freely dissociable IGF-1 protein levels in undernourished EtOH-fed dams. The liver is the major source (75%–80%) of IGF-1 in the general circulation (38, 39). It is likely, therefore, that a 50% decrease in hepatic IGF-1 mRNA in the undernourished EtOH dams is responsible for the reduced serum IGF-1 levels. However, it is not clear what degree of IGF-1 decrease in the circulation of the dam is required for fetal growth retardation.

IGF binding proteins (IGFBPs) control the minute-to-minute bioavailability and tissue-targeting of IGF-1 (40). Circulating IGF-1 is mainly found complexed to either IGFBP-3 or IGFBP-1 (41). Consistent with our data, previous studies have shown induction of IGFBP-1 by EtOH (18). This increase in IGFBP-1 may be mediated by tumor necrosis factor-α (41). It is interesting to note that IGFBP-1 and -2 levels were induced following reduced caloric intake. IGF-1 gene expression is controlled by growth hormone (GH) levels (18). Chronic EtOH-infusion decreases GH levels (10) and suppresses STAT5b expression in male rats (43). Since the present studies demonstrated decreased IGF-1 gene expression, we investigated GH signaling and found that the combination of EtOH and undernutrition decreased STAT5b protein and mRNA in pregnant rats. Since Woelfle *et al.* (22) recently implied that IGF-1 gene expression is acutely controlled by GH through STAT5b, our data suggest that reduced STAT5b may mediate the decrease in IGF-1 gene expression. Srivastava *et al.* (44), using rats overexpressing bovine GH, reported that EtOH-induced suppression of IGF-1 gene expression was dependent on post-GH-receptor signaling mechanisms. Our data are consistent with these findings and suggest that the post-GH-receptor events, such as decreased STAT5b activation or transcription, may be involved. To our knowledge, this is the first report to demonstrate interactive effects of EtOH and nutrition on STAT5 mRNA levels. However, the mechanisms behind EtOH-induced decreased STAT5b mRNA levels in undernourished EtOH dams require further study.

The present data address the question of whether EtOH and undernutrition affect fetal circulating (serum) IGF-1 levels in relation to fetal growth. Elegant studies by Yakar *et al.* (39) suggest that even in the complete absence of maternal hepatic IGF-1, other sources of IGF-1, such as the adipose tissue, kidney, and uterus, can sustain normal fetal growth. The evidence on modulation of fetal IGF-1 levels by EtOH is split, as Singh *et al.* (45) found modest (17%) decrease in serum IGF-1 in fetuses of EtOH-fed dams and Mauceri *et al.* (46) found no change in circulating fetal IGF-1 levels. Our data are consistent with the findings of Mauceri *et al.* (46). However, in agreement with the modulation of IGFBPs in the maternal liver, fetal livers also showed an increase in IGFBP-1 and -2. These data raise the possibility that increased IGFBP-1 levels in the dam and the fetus may cause growth retardation in an IGF-1-independent fashion. This possibility has been studied in transgenic-mice overexpressing hIGFBP-1, specifically in the maternal decidua (47).

IGF-1 and -2 and IGFBPs have important roles in feto-placental development and growth (48, 49). Chronic EtOH exposure has significant adverse effects on placental morphology and function. Abnormal trophoblast invasion in decidua, nuclear disorder in trophoblastic giant cells, derangement in the labyrinth, changes in blood sinuses, and extracellular matrix deposition have been recently described (50). Further, EtOH inhibits IGF-1-stimulated amino acid uptake in human placental trophoblasts (51). Since fetal growth retardation in the EtOH-undernutrition combination occurs in the absence of changes in fetal IGF-1, this is consistent with the hypothesis that EtOH-induced fetal growth retardation occurs primarily as a result of impaired placental development and transport of nutrients resulting primarily from disruption of maternal GH-IGF axis.

In addition, other mechanisms involving induced MT-2 expression in the 160 EtOH group, as observed by real-time RT-PCR, may alter maternal-fetal zinc homeostasis and lead to fetal growth retardation. Metallothionein overexpression protects against EtOH-induced liver damage, oxidative stress, and apoptosis (52, 53). Zinc treatment in MT-knockout mice also attenuates EtOH-induced liver necrosis *via* its antioxidant properties (54, 55). Further, in a murine model of intraperitoneal EtOH challenge on GD8, fetal zinc transfer was impaired in WT but not in MT-knockout mice, linking MT-induction to impairment of maternal-fetal zinc transfer (56). Using the same model, supplementation of zinc ameliorated both overt EtOH-induced fetal tertogenicity and spatial memory impairments in the offspring (57, 58). It is likely that the marked induction of MT genes in 160 EtOH group (over that of the undernutrition effect

itself) has important mechanistic implications that remain to be examined.

In conclusion, we report marked enhancement of EtOH metabolism in pregnancy, an effect abolished by undernutrition due to suppression of maternal ADH-1. Consistent with higher UECs, fetuses from undernourished EtOH-fed dams suffered higher toxicity. Hepatic IGF-1 mRNA and serum IGF-1 levels were downregulated in undernourished EtOH-fed dams accompanied with increased IGFBP-1 and -2 gene expression and decreased STAT5b protein and gene expression. Undernutrition appears to be a significant risk factor in EtOH-associated fetal growth retardation, which may be in part due to the altered maternal hepatic gene expression profile. The data suggest that optimal nutritional management during pregnancy may be an effective way to reduce the penetrance of fetal alcohol toxicity in high-risk individuals.

We thank Brandi Yarberry, Janelle C. Johnson, Ying Chen, Matt Ferguson, Tammy Dallari, Pamela Treadaway, and Michele Perry for their technical assistance.

1. Randall CL. Alcohol and pregnancy: highlights from three decades of research. J Stud Alcohol 62:554–561, 2001.
2. Eustace LW, Kang DH, Coombs D. Fetal alcohol syndrome: a growing concern for health care professionals. J Obstet Gynecol Neonatal Nurs 32:215–221, 2003.
3. Jacobson JL, Jacobson SW, Sokol RJ, Ager JW Jr. Relation of maternal age and pattern of pregnancy drinking to functionally significant cognitive deficit in infancy. Alcohol Clin Exp Res 22:345–351, 1998.
4. Dreosti IE. Nutritional factors underlying the expression of the fetal alcohol syndrome. Ann N Y Acad Sci 678:193–204, 1993.
5. Stewart DE, Streiner D. Alcohol drinking in pregnancy. Gen Hosp Psychiatry 16:406–412, 1994.
6. Goad PT, Hill DE, Slikker W Jr., Kimmel CA, Gaylor DW. The role of maternal diet in the developmental toxicology of ethanol. Toxicol Appl Pharmacol 73:256–267, 1984.
7. Tsukamoto H, French SW. Evolution of intragastric ethanol infusion model. Alcohol 10:437–441, 1993.
8. Wiener SG, Shoemaker WJ, Koda LY, Bloom FE. Interaction of ethanol and nutrition during gestation: influence on maternal and offspring development in the rat. J Pharmacol Exp Ther 216:572–579, 1981.
9. Breese CR, D'Costa A, Ingram RL, Lenham J, Sonntag WE. Long-term suppression of insulin-like growth factor-1 in rats after in utero ethanol exposure: relationship to somatic growth. J Pharmacol Exp Ther 264: 448–456, 1993.
10. Badger TM, Ronis MJ, Lumpkin CK, Valentine CR, Shahare M, Irby D, Huang J, Mercado C, Thomas P, Ingelman-Sundberg M, . Effects of chronic ethanol on growth hormone secretion and hepatic cytochrome P450 isozymes of the rat. J Pharmacol Exp Ther 264:438–447, 1993.
11. Badger TM, Crouch J, Irby D, Hakkak R, Shahare M. Episodic excretion of ethanol during chronic intragastric ethanol infusion in the male rat: continuous vs. cyclic ethanol and nutrient infusions. J Pharmacol Exp Ther 264:938–943, 1993.
12. Ronis MJ, Lumpkin CK, Ingelman-Sundberg M, Badger TM. Effects of short-term ethanol and nutrition on the hepatic microsomal monooxygenase system in a model utilizing total enteral nutrition in the rat. Alcohol Clin Exp Res 15:693–699, 1991.
13. Badger TM, Hidestrand M, Shankar K, McGuinn WD, Ronis MJ. The effects of pregnancy on ethanol clearance. Life Sci 77:2111–2116, 2005.
14. Lumeng L, Bosron WF, Li TK. Rate-determining factors for ethanol metabolism in vivo during fasting. Adv Exp Med Biol 132:489–496, 1980.
15. Johansson I, Ingelman-Sundberg M. Carbon tetrachloride-induced lipid peroxidation dependent on an ethanol-inducible form of rabbit liver microsomal cytochrome P-450. FEBS Lett 183:265–269, 1985.
16. He L, Ronis MJ, Badger TM. Ethanol induction of class I alcohol dehydrogenase expression in the rat occurs through alterations in CCAAT/enhancer binding proteins beta and gamma. J Biol Chem 277: 43572–43577, 2002.
17. Eisen MB, Spellman PT, Brown PO, Botstein D. Cluster analysis and display of genome-wide expression patterns. Proc Natl Acad Sci U S A 95:14863–14868, 1998.
18. Lang CH, Liu X, Nystrom G, Wu D, Cooney RN, Frost RA. Acute effects of growth hormone in alcohol-fed rats. Alcohol Alcohol 35: 148–158, 2000.
19. Boyne MS, Thame M, Bennett FI, Osmond C, Miell JP, Forrester TE. The relationship among circulating insulin-like growth factor (IGF)-I, IGF-binding proteins-1 and –2, and birth anthropometry: a prospective study. J Clin Endocrinol Metab 88:1687–1691, 2003.
20. Diaz E, Halhali A, Luna C, Diaz L, Avila E, Larrea F. Newborn birth weight correlates with placental zinc, umbilical insulin-like growth factor I, and leptin levels in preeclampsia. Arch Med Res 33:40–47, 2002.
21. Liu HC, He ZY, Mele CA, Veeck LL, Davis OK, Rosenwaks Z. Expression of IGFs and their receptors is a potential marker for embryo quality. Am J Reprod Immunol 38:237–245, 1997.
22. Woelfle J, Billiard J, Rotwein P. Acute control of insulin-like growth factor-I gene transcription by growth hormone through Stat5b. J Biol Chem 278:22696–22702, 2003.
23. Badger TM, Hoog JO, Svensson S, McGehee RE Jr, Fang C, Ronis MJ, Ingelman-Sundberg M. Cyclic expression of class I alcohol dehydrogenase in male rats treated with ethanol. Biochem Biophys Res Commun. 274:684–688, 2000.
24. He L, Simmen FA, Ronis MJ, Badger TM. Post-transcriptional regulation of sterol regulatory element-binding protein-1 by ethanol induces class I alcohol dehydrogenase in rat liver. J Biol Chem 279: 28113–28121, 2004.
25. Matsumoto H, Fujimiya T, Fukui Y. Role of alcohol dehydrogenase in rat ethanol elimination kinetics. Alcohol Alcohol 29:15–20, 1994.
26. Teschke R, Gellert J. Hepatic microsomal ethanol-oxidizing system (MEOS): metabolic aspects and clinical implications. Alcohol Clin Exp Res 10:20S–32S, 1986.
27. Bosron WF, Crabb DW, Housinger TA, Li TK. Effect of fasting on the activity and turnover of rat liver alcohol dehydrogenase. Alcohol Clin Exp Res 8:196–200, 1984.
28. Feuers RJ, Duffy PH, Leakey JA, Turturro A, Mittelstaedt RA, Hart RW. Effect of chronic caloric restriction on hepatic enzymes of intermediary metabolism in the male Fischer 344 rat. Mech Ageing Dev 48:179–189, 1989.
29. Lumeng L, Bosron WF, Li TK. Quantitative correlation of ethanol elimination rates in vivo with liver alcohol dehydrogenase activities in fed, fasted and food-restricted rats. Biochem Pharmacol 28:1547–1551, 1979.
30. Crabb DW, Matsumoto M, Chang D, You M. Overview of the role of alcohol dehydrogenase and aldehyde dehydrogenase and their variants in the genesis of alcohol-related pathology. Proc Nutr Soc 63:49–63, 2004.
31. Potter JJ, Mezey E. Effect of STAT5b on rat liver alcohol dehydrogenase. Arch Biochem Biophys 391:41–48, 2001.
32. Roesler WJ. The role of C/EBP in nutrient and hormonal regulation of gene expression. Annu Rev Nutr 21:141–165, 2001.
33. Klarlund JK, Czech MP. Insulin-like growth factor I and insulin rapidly

increase casein kinase II activity in BALB/c 3T3 fibroblasts. J Biol Chem 263:15872–15875, 1988.

34. Miell JP, Marway JS, Jones J, Preedy VR. The effects of acute administration of ethanol on jejunal protein synthesis and circulating insulin-like growth factor (IGF)-1 and IGF binding proteins in ad libitum fed and nutritionally restricted rats. Addict Biol 1:371–378, 1996.
35. Rojdmark S, Brismar K. Decreased IGF-I bioavailability after ethanol abuse in alcoholics: partial restitution after short-term abstinence. J Endocrinol Invest 24:476–482, 2001.
36. Resnicoff M, Sell C, Ambrose D, Baserga R, Rubin R. Ethanol inhibits the autophosphorylation of the insulin-like growth factor 1 (IGF-1) receptor and IGF-1-mediated proliferation of 3T3 cells. J Biol Chem 268:21777–21782, 1993.
37. Breese CR, Sonntag WE. Effect of ethanol on plasma and hepatic insulin-like growth factor regulation in pregnant rats. Alcohol Clin Exp Res 19:867–873, 1995.
38. Liu JL, Yakar S, LeRoith D. Conditional knockout of mouse insulin-like growth factor-1 gene using the Cre/loxP system. Proc Soc Exp Biol Med 223:344–351, 2000.
39. Yakar S, Liu JL, Stannard B, Butler A, Accili D, Sauer B, LeRoith D. Normal growth and development in the absence of hepatic insulin-like growth factor I. Proc Natl Acad Sci U S A 96:7324–7329, 1999.
40. Huang ST, Vo KC, Lyell DJ, Faessen GH, Tulac S, Tibshirani R, Giaccia AJ, Giudice LC. Developmental response to hypoxia. FASEB J 18:1348–1365, 2004.
41. Monzavi R, Cohen P. IGFs and IGFBPs: role in health and disease. Best Pract Res Clin Endocrinol Metab 16:433–447, 2002.
42. Kumar V, Silvis C, Nystrom G, Deshpande N, Vary TC, Frost RA, Lang CH. Alcohol-induced increases in insulin-like growth factor binding protein-1 are partially mediated by TNF. Alcohol Clin Exp Res 26:1574–1583, 2002.
43. Badger TM, Ronis MJ, Frank SJ, Chen Y, He L. Effects of chronic ethanol on hepatic and renal CYP2C11 in the male rat: interactions with the Janus-kinase 2-signal transducer and activators of transcription proteins 5b pathway. Endocrinology 144:3969–3976, 2003.
44. Srivastava VK, Dearth RK, Hiney JK, Chandrashekar V, Mattison JA, Bartke A, Dees WL. Alcohol suppresses insulin-like growth factor-1 gene expression in prepubertal transgenic female mice overexpressing the bovine growth hormone gene. Alcohol Clin Exp Res 26:1697–1702, 2002.
45. Singh SP, Srivenugopal KS, Ehmann S, Yuan XH, Snyder AK. Insulin-like growth factors (IGF-I and IGF-II), IGF-binding proteins, and IGF gene expression in the offspring of ethanol-fed rats. J Lab Clin Med 124:183–192, 1994.
46. Mauceri HJ, Unterman T, Dempsey S, Lee WH, Conway S. Effect of ethanol exposure on circulating levels of insulin-like growth factor I and II, and insulin-like growth factor binding proteins in fetal rats. Alcohol Clin Exp Res 17:1201–1206, 1993.
47. Crossey PA, Pillai CC, Miell JP. Altered placental development and intrauterine growth restriction in IGF binding protein-1 transgenic mice. J Clin Invest 110:411–418, 2002.
48. Fowden AL. The insulin-like growth factors and feto-placental growth. Placenta 24:803–812, 2003.
49. Jones JI, Clemmons DR. Insulin-like growth factors and their binding proteins: biological actions. Endocr Rev 16:3–34, 1995.
50. Turan AM, Arzu KE. The effects of alcohol on rat placenta. Cell Biochem Funct 23:435–445, 2005.
51. Karl PI, Fisher SE. Chronic ethanol exposure inhibits insulin and IGF-1 stimulated amino acid uptake in cultured human placental trophoblasts. Alcohol Clin Exp Res 18:942–946, 1994.
52. Zhou Z, Sun X, James Kang Y. Metallothionein protection against alcoholic liver injury through inhibition of oxidative stress. Exp Biol Med 227:214–222, 2002.
53. Lambert JC, Zhou Z, Kang YJ. Suppression of Fas-mediated signaling pathway is involved in zinc inhibition of ethanol-induced liver apoptosis. Exp Biol Med 228:406–412, 2003.
54. Zhou Z, Sun X, Lambert JC, Saari JT, Kang YJ. Metallothionein-independent zinc protection from alcoholic liver injury. Am J Pathol 160:2267–2274, 2002.
55. Zhou Z, Wang L, Song Z, Saari JT, McClain CJ, Kang YJ. Zinc supplementation prevents alcoholic liver injury in mice through attenuation of oxidative stress. Am J Pathol 166:1681–1690, 2005.
56. Carey LC, Coyle P, Philcox JC, Rofe AM. Maternal ethanol exposure is associated with decreased plasma zinc and increased fetal abnormalities in normal but not metallothionein-null mice. Alcohol Clin Exp Res. 24:213–219, 2000.
57. Carey LC, Coyle P, Philcox JC, Rofe AM. Zinc supplementation at the time of ethanol exposure ameliorates teratogenicity in mice. Alcohol Clin Exp Res 27:107–110, 2003.
58. Summers BL, Rofe AM, Coyle P. Prenatal zinc treatment at the time of acute ethanol exposure limits spatial memory impairments in mouse offspring. Pediatr Res 59:66–71, 2006.